

A NEW DETECTOR FOR CHANNELS WITH STATE
VARIABLE MODELS

A THESIS

Presented to

The Faculty of the Division of Graduate
Studies and Research

by

John Kenna Roach, III

In Partial Fulfillment
of the Requirements for the Degree
Doctor of Philosophy
in the School of Electrical Engineering

Georgia Institute of Technology

December, 1974

A NEW DETECTOR FOR CHANNELS WITH STATE
VARIABLE MODELS

Approved:

James E. Brown, III, Chairman

Aubrey M. Fish

Ray H. Pettit

Date approved by Chairman: Nov. 20, 1974

ACKNOWLEDGMENTS

To Dr. James E. Brown, III, my thesis advisor, I would like to express my sincerest appreciation for his guidance and encouragement throughout the development of this dissertation. I would also like to thank Dr. A. M. Bush and Dr. R. H. Pettit for serving on my reading committee and for fundamentally educating me in the field of communications.

I also express special appreciation to my wife, Judy, for her patience and encouragement that made this thesis possible.

TABLE OF CONTENTS

	Page
ACKNOWLEDGMENTS.	ii
LIST OF ILLUSTRATIONS.	v
SUMMARY.	vii
Chapter	
I. INTRODUCTION.	1
Problem Description and Contribution.	1
History of the Problem.	2
Outline of the Dissertation	5
II. DERIVATION OF THE MATHEMATICAL MODEL.	6
Introduction.	6
Derivation of the Equations for State	
Variable Channels	12
Derivation of the Equations for FDIR	
Channels.	16
III. DEVELOPMENT OF THE ESTIMATE FEEDBACK	
DETECTOR.	21
Introduction.	21
Development of the Estimate Feedback	
Detector for FDIR Channels.	22
Development of the Estimate Feedback	
Detector for State Variable Channels.	26
Comparison of the A-F Detector with the	
Viterbi Detector.	33
An Error Rate Estimate.	34
IV. RESULTS OF THE COMPUTER SIMULATIONS	35
Introduction.	35
Presentation of Monte Carlo Results	37
V. CONCLUSIONS AND RECOMMENDATIONS	52
Conclusions	52
Recommendations	53

TABLE OF CONTENTS (Concluded)

Appendices	Page
A. SUFFICIENT STATISTICS FOR THE INTERSYMBOL INTERFERENCE PROBLEM.	54
Introduction.	54
Sufficient Statistics for State Variable Channels.	56
Sufficient Statistics for FDIR Channels	59
B. PROBABILITY OF ERROR FOR THE OPTIMUM DETECTOR.	61
C. THE ESTIMATE FEEDBACK ALGORITHM	63
BIBLIOGRAPHY	67
VITA	70

LIST OF ILLUSTRATIONS

Figure		Page
1.	Functional Block Diagram of a Digital Communication System.	7
2.	Low Pass Equivalent Block Diagram of a Digital Communication System.	8
3.	Hard Decision Directed Binary Detector for FDIR Channels	25
4.	Soft Decision Directed Binary Detector for FDIR Channels	25
5.	Estimate Feedback Binary Detector for FDIR Channels.	27
6.	Hard Decision Directed Binary Detector for State Variable Channels	30
7.	Soft Decision Directed Binary Detector for State Variable Channels	30
8.	Estimate Feedback Binary Detector for State Variable Channels	32
9.	Error Rate of a One Pole Butterworth Filter Channel with $f_{co} = 1/2\pi$ and $T = 1$	38
10.	Error Rate of a Two Pole Butterworth Filter Channel with $f_{co} = .5$ and $T = 1$	41
11.	Monte Carlo Error Rate for Abend-Fritchman Channel Model, $D = 0$	43
12.	Monte Carlo Error Rate for Abend-Fritchman Channel Model, $D = 1$	44
13.	Monte Carlo Error Rate for Abend-Fritchman Channel Model, $D = 2$	45
14.	Monte Carlo Error Rate for Abend-Fritchman Channel Model, $D = 3$	46

LIST OF ILLUSTRATIONS (Concluded)

Figure		Page
15.	Monte Carlo Error Rate for Abend-Fritchman Channel Model, $D = 4$	47
16.	Monte Carlo Error Rate for Abend-Fritchman Channel Model, $D = 5$	48
17.	Monte Carlo Error Rates for One Pole Butterworth Channel Model with $f_{co} = 1/2\pi$ and $T = 1$; Comparative Results for a Number of Detectors	49
18.	Monte Carlo Error Rates for Two Pole Butterworth Channel Model with $f_{co} = .5$ and $T = 1$; Comparative Results for a Number of Detectors	50

SUMMARY

In this dissertation a new suboptimum intersymbol interference detector is developed that could be applied to channels whose memory is represented either by a finite duration impulse response model or by a state variable model. The detector utilizes channel state estimates to reduce computational complexity and also generates, at little additional cost, an estimate of error rate.

A set of discrete time state and observation equations, representing the functional relationship between the information bit stream and the sequence of observations, is derived for use in the detector algorithm. This derivation holds for any modulation/demodulation scheme which can be represented by signal space techniques, for any set of linear receiver sampling filters, and for any linear, time-varying bandpass channel filter. In addition, a set of sufficient statistics for bandpass channels whose memory is represented by linear, time-invariant state variable models is defined.

Monte Carlo simulation results for the new detector are reported on and show that for three specific channel models the new detector performs close to the optimum detector performance but is considerably less complex.

CHAPTER I

INTRODUCTION

Problem Description and Contribution

The problem of limited available spectrum has in recent years forced digital communication system designers to attempt to transmit over their allocated channels at higher and higher symbol rates and cope with intersymbol interference. This has made the tradeoff of higher signaling rate for increased receiver complexity appear more and more attractive [9,10,15,16,19,20].

For the case of linear dispersive channels considered here, the underlying cause of the intersymbol interference problem can be described in either the frequency or time domain. From a frequency domain viewpoint, intersymbol interference occurs either because the amplitude response of the channel filter is not flat or because the phase characteristic is not linear over the frequency band occupied by the spectrum of the signaling pulse.

From a time domain viewpoint, the problem occurs because the impulse response, which indicates the memory of the channel, has a duration on the order of a signaling interval or longer. The channel output, obtained by convolving the channel impulse response with the signaling pulse, thus lasts significantly beyond the signaling interval.

In most previous research a time domain viewpoint has proven valuable. Two canonic channel models have been used--a finite duration

impulse response (FDIR) model [1,2,3,4,5,6,8,9,10,12,13,15,16,17,18,19, 20,21,22] and a continuous time state variable model [11]. A time domain approach has been taken in this report and the techniques developed can be used with either model. The discrete time recursive equations which relate the observation to the input symbol and which form a part of the detector algorithm unify the two approaches to channel modeling.

Specifically, the contributions of this research are:

1. The development of a new suboptimum intersymbol interference detector using state estimates to reduce computational complexity and generating, at little additional cost, a measure of error rate.

2. The derivation of a set of discrete time state and observation equations, representing the functional relationship between the information bit stream and the sequence of observations given to the detector. The derivation holds for any modulation/demodulation scheme which can be represented by signal space techniques; for any set of receiver sampling filters, matched or not; and for any linear, time-varying bandpass channel filter, either symmetric or unsymmetric about the carrier.

3. The derivation of a set of sufficient statistics for bandpass channels whose memory is modeled by linear, time-invariant state variable models. A derivation for FDIR channels is also developed for completeness but Forney [16] has previously considered this case.

History of the Problem

Probably the earliest approach to amelioration of the intersymbol interference problem in digital communications was to view the problem in the frequency domain and to correct for nonideal frequency characteristics

of the channel by means of fixed compensators. Correction of amplitude response was emphasized over correction of phase response. This method proved to be adequate for speech transmission.

With the advent of high speed data transmission, more stringent requirements were placed on digital communication systems. To meet these needs, a number of different approaches were taken in designing more sophisticated receivers [1-22]. These approaches can be conveniently classified as linear or nonlinear processors of the observed noisy samples.

Linear Detectors

The linear intersymbol interference detector that optimizes almost any reasonable criterion, such as probability of error, or mean square error, was shown by Ericson [1] to have a certain canonic structure. This structure consists of a filter matched to the channel output pulse followed by an infinite length transversal filter whose tap delay is equal to the signaling interval.

Aaron and Tufts [2] specified the number of delay elements in the filter and obtained the optimal tap gains as solutions of a set of nonlinear equations. Recently Lawrence and Kaufman [3] assumed a discrete time state variable (delay line) model for the channel and used a Kalman filter to estimate the channel state from noisy measurements. Berger and Tufts [4] compared performance of their detector with the rate distortion bound and found that the suboptimality of m.m.s.e. linear detectors was pronounced at high SNR since performance improved as the reciprocal of SNR rather than exponentially. Additional references, which present work very similar to that listed above, are [5,6,7,8].

Nonlinear Detectors

It became apparent, after experiments with linear detectors, that detectors for intersymbol interference channels which could operate well at high SNR would have to be nonlinear [4]. Chang and Hancock [9] were the first to publish a deeper recognition of the underlying statistics of the problem. They developed the Bayes detector that assumed a channel impulse response of finite length and made a decision concerning a block of symbols.

Several approaches have been considered for reducing the complexity of the optimum detector. Austin [10] considered approximating the maximum likelihood (ML) detector by feeding back previous decisions as if they were errorless. His detector was developed for FDIR channel models and consisted of a matched filter followed by a feedback loop with two transversal filters. The forward line acted in the same manner as earlier equalizers, and the feedback path filtered previous decisions. Bershad and Vena [11] also used a hard decision directed (HDD) approach for channels with state variable models but considered only the realizable case.

A simple soft decision directed (SDD) approach was used by Taylor [12,13] to obtain better results than those for an HDD detector. Here the hard decision was put through a nonlinearity such as the hyperbolic tangent to generate a hedged decision for feedback. The relationship between Taylor's work and earlier research by J. W. Mark is described in [14].

Neither of the approximate detectors listed above was operated

with delay nor did they approximate the optimum MAP detection algorithm. In order to achieve good results at moderate-to-low SNR, more complex algorithms were necessary. Abend and Fritchman [15] developed a minimum probability of symbol error detector that was realizable with a delay of D signaling intervals and was optimum in the limit as D increased. Forney [16] developed an ML receiver employing the Viterbi algorithm as the nonlinear processor. The Viterbi algorithm is optimum for making sequence decisions if delay is infinite; however, for finite D it is suboptimum. Both Abend and Fritchman and Forney assumed an FDIR channel model.

Other references are [17,18,19,20,21,22]. These are included in the list of references for completeness but report on detectors of the same form as those mentioned above.

Outline of the Dissertation

In Chapter II the class of problems addressed in this dissertation is defined, and two sets of discrete time equations, used in the new detector algorithm, are derived from continuous time channel models.

Chapter III discusses three canonic approaches to the design of nonlinear detectors for the intersymbol interference problem. A description is given of the advantages of the detector presented here.

In Chapter IV results of the Monte Carlo simulation of three different channel models are presented, along with comparisons of the results for the detectors developed here and a number of detectors mentioned in Chapter III.

Chapter V summarizes the conclusions resulting from this research and presents recommendations for extensions to the work.

CHAPTER II

DERIVATION OF THE MATHEMATICAL MODEL

Introduction

In this chapter the discrete time equations that relate the information symbol to the channel state vector and to the observation vector are developed. The derivation postulates the Hilbert space representation of the signaling waveforms and the complex envelope representation for the bandpass channel filtering, and, after a series of conceptually simple manipulations, the required equations are obtained.

Sets of equations for both a state variable channel model and for an FDIR channel model are obtained. (Some special cases for the FDIR channel model are given in [15] and [21].) The observation vector can be generated by sampling a bank of matched filters, a bank of suboptimum filters, or the incoming waveform without filtering. A set of optimum filters is derived in Appendix A.

A functional block diagram of the class of digital communication systems considered in this research is shown in Figure 1. The functions are defined so that correspondences between Figure 1 and the low-pass equivalent block diagram in Figure 2 can easily be seen.

The M-ary information source sends to the baseband modulator an M-dimensional vector, $\underline{u}_k \in \{\underline{A}_1, \underline{A}_2, \dots, \underline{A}_M\}$, whose components are the coordinates of the k^{th} signaling pulse. The baseband modulator selects

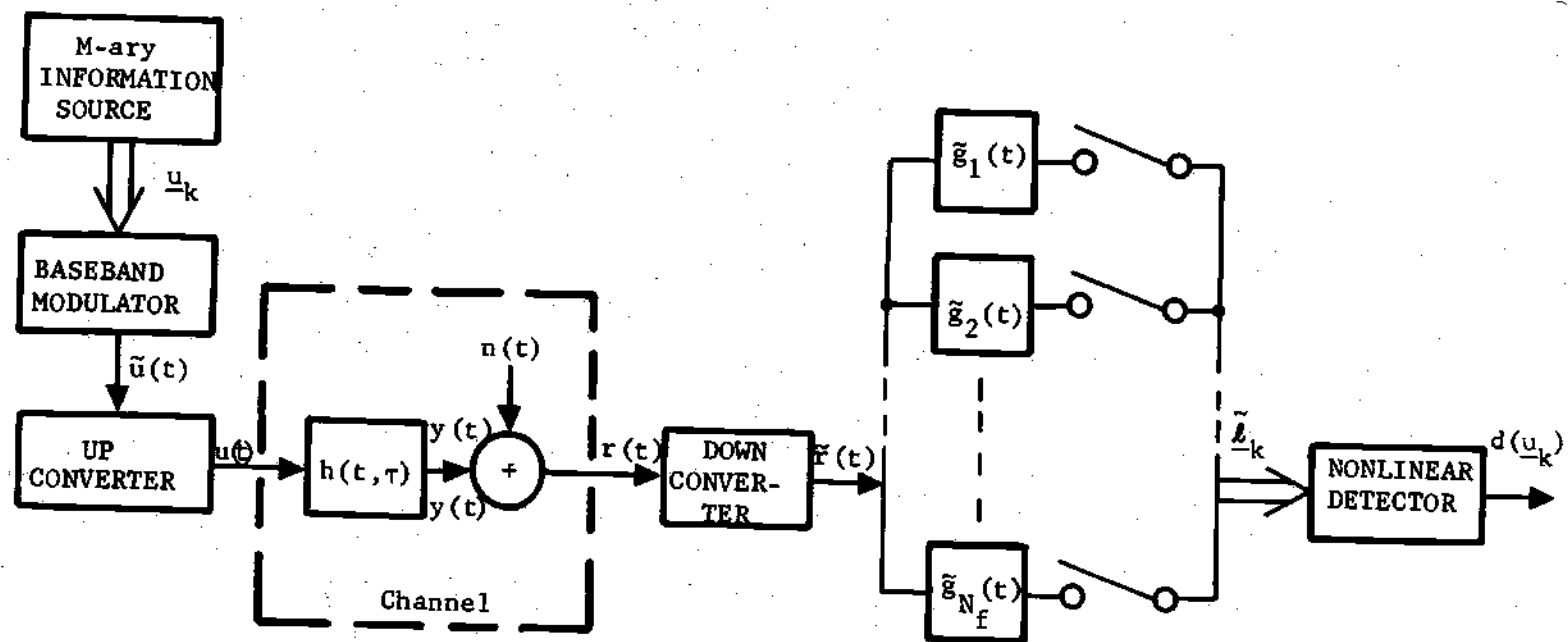


Figure 1. Functional Block Diagram of a Digital Communication System

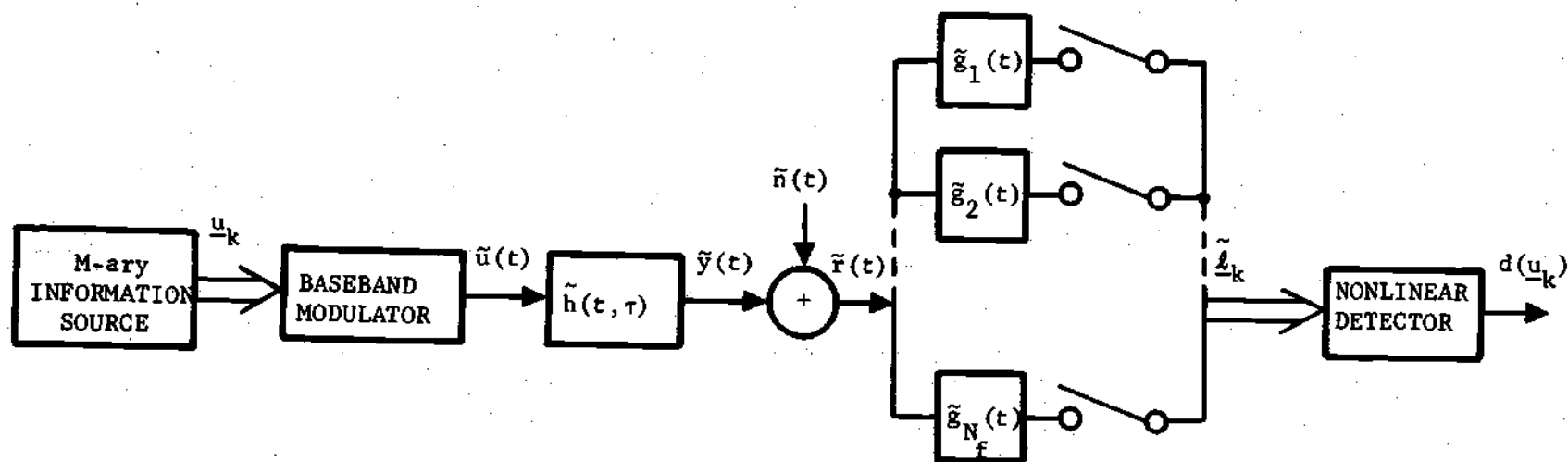


Figure 2. Low Pass Equivalent Block Diagram of a Digital Communication System

the corresponding waveform $\tilde{u}(t)$ by an operation which can be represented as

$$\tilde{u}(t) = \tilde{\Phi}'(t - (k-1)T) \underline{u}_k \quad (k-1)T < t < kT \quad (2.1)$$

where $\tilde{\Phi}(t)$ is a vector whose components form a basis set for the complex signal space, T is the signaling interval, and the prime denotes matrix transpose. $\tilde{\Phi}(t)$ contains information on both the modulation used, e.g., ASK, PSK, or FSK, and on the basic signaling pulse shape, e.g., NRZ or split phase. The upconverter generates the RF pulse

$$u(t) = \text{Re} \{ \tilde{u}(t) e^{j\omega_c t} \} . \quad (2.2)$$

The channel produces an RF output,

$$r(t) = y(t) + n(t) , \quad (2.3)$$

and the downconverter generates

$$\tilde{r}(t) = \text{Re} \{ r(t) e^{-j\omega_c t} \} . \quad (2.4)$$

This complex waveform is then filtered by the bank of filters $\{\tilde{g}_i(t)\}$ to generate the observation vector, $\tilde{\underline{z}}_k$.

To illustrate the model, parameters for BPSK and QPSK are given below:

BPSK: $M = 2$

$$\underline{u}_k \in \left\{ \begin{bmatrix} 1 \\ 0 \end{bmatrix}, \begin{bmatrix} 0 \\ 1 \end{bmatrix} \right\}$$

$$\tilde{\Phi}(t) = \begin{bmatrix} e^{j\pi/2} \\ e^{-j\pi/2} \end{bmatrix}, \quad 0 < t < T$$

$$\tilde{u}(t) = \tilde{\Phi}'(t) \underline{u}_k = \begin{bmatrix} e^{j\pi/2} & e^{-j\pi/2} \end{bmatrix} \underline{u}_k$$

$$u(t) = \text{Re} \{ \tilde{u}(t) e^{j\omega_c t} \} = \text{Re} \left\{ \begin{bmatrix} e^{j(\omega_c t + \pi/2)} & e^{j(\omega_c t - \pi/2)} \end{bmatrix} \underline{u}_k \right\}$$

$$= \begin{bmatrix} \cos(\omega_c t + \pi/2) & \cos(\omega_c t - \pi/2) \end{bmatrix} \underline{u}_k$$

QPSK: $M = 4$

$$\underline{u}_k \in \left\{ \begin{bmatrix} 1 \\ 0 \\ 0 \\ 0 \end{bmatrix}, \begin{bmatrix} 0 \\ 1 \\ 0 \\ 0 \end{bmatrix}, \begin{bmatrix} 0 \\ 0 \\ 1 \\ 0 \end{bmatrix}, \begin{bmatrix} 0 \\ 0 \\ 0 \\ 1 \end{bmatrix} \right\}$$

$$\tilde{\Phi}(t) = \begin{bmatrix} e^{j\pi/2} \\ e^{j\pi} \\ e^{j3\pi/2} \\ e^{j2\pi} \end{bmatrix}, \quad 0 < t < T$$

$$\tilde{u}(t) = \tilde{\Phi}'(t) \underline{u}_k = \begin{bmatrix} e^{j\pi/2} & e^{j\pi} & e^{j3\pi/2} & e^{j2\pi} \end{bmatrix} \underline{u}_k$$

$$u(t) = \text{Re} \{ \tilde{u}(t) e^{j\omega_c t} \}$$

$$= \begin{bmatrix} \cos(\omega_c t + \pi/2) & \cos(\omega_c t + \pi) & \cos(\omega_c t + 3\pi/2) & \cos(\omega_c t + 2\pi) \end{bmatrix} \underline{u}_k$$

Under the assumption that the RF carrier component is much larger than any significant components of the baseband modulator output, the model in Figure 1 may be replaced by the complex low-pass equivalent model shown in Figure 2. This is the specific model used in this chapter in the derivation of the discrete time state equations.

In addition to the above the following assumptions are made in the derivation:

1. The sequence $u_k = \{u_i\}_{i=1}^k$ is a statistically independent sequence.
2. $\tilde{n}(t)$ is complex WGN with spectral density N_0 .
3. The receiver has exact knowledge of the RF carrier frequency and phase.
4. The receiver has exact knowledge of bit timing.
5. Each of the receiver filters is dumped after the output is sampled.
6. All channel filter parameters are known.

These assumptions are warranted in order to limit to manageable proportions the scope of this research.

The output of the baseband modulator can be written

$$\tilde{u}(t) = \sum_{j=1}^k \tilde{\Phi}'(t-(j-1)T) \underline{u}_j \quad 0 < t < kT \quad (2.5)$$

Under the assumption of a high frequency carrier, the complex envelope of the channel filter output can be written

$$\tilde{y}(t) = \int_0^t \tilde{h}(t, \tau) \tilde{u}(\tau) d\tau \quad (2.6)$$

where

$$h(t, \tau) = \operatorname{Re} \{ \tilde{h}(t, \tau) e^{j\omega_c(t-\tau)} \} . \quad (2.7)$$

Now a specific channel model must be chosen.

Derivation of the Equations for State Variable Channels

Assume that the dynamic behavior of the filter portion of the channel can be represented by

$$\dot{\underline{\tilde{x}}}(t) = \tilde{F}_c(t) \underline{\tilde{x}}(t) + \tilde{G}_c(t) \tilde{u}(t) \quad (2.8)$$

$$\tilde{y}(t) = \tilde{H}_c(t) \underline{\tilde{x}}(t) , \quad (2.9)$$

where $\underline{\tilde{x}}(t)$ is the complex state of the filter.

A discrete time state equation can be obtained by writing the complete solution to the continuous time state equation, with $\tilde{\phi}$ being the state transition matrix,

$$\underline{\tilde{x}}(t) = \tilde{\phi}(t, t_1) \underline{\tilde{x}}(t_1) + \int_{t_1}^t \tilde{\phi}(t, \tau) \tilde{G}_c(\tau) \tilde{u}(\tau) d\tau , \quad (2.10)$$

and setting $t_1 = (k-1)T$ and $t = kT$, so that

$$\underline{\tilde{x}}_k = \underline{\tilde{x}}(kT) = \tilde{\phi}(kT, (k-1)T) \underline{\tilde{x}}_{k-1} + \int_{(k-1)T}^{kT} \tilde{\phi}(kT, \tau) \tilde{G}_c(\tau) \tilde{u}(\tau) d\tau . \quad (2.11)$$

Substituting (2.5) into the above gives

$$\underline{\tilde{x}}_k = \tilde{\phi}(kT, (k-1)T) \underline{\tilde{x}}_{k-1} + \int_{(k-1)T}^{kT} \tilde{\phi}(kT, \tau) \tilde{\underline{G}}_c(\tau) \tilde{\underline{\psi}}'(\tau - (k-1)T) d\tau \underline{u}_k. \quad (2.12)$$

The change of variables,

$$\tau_1 = \tau - (k-1)T,$$

in (2.12) gives

$$\underline{\tilde{x}}_k = \tilde{\phi}(kT, (k-1)T) \underline{\tilde{x}}_{k-1} + \int_0^T \tilde{\phi}(kT, \tau_1 + (k-1)T) \tilde{\underline{G}}_c(\tau_1 + (k-1)T) \tilde{\underline{\psi}}'(\tau_1) d\tau_1 \underline{u}_k. \quad (2.13)$$

By defining

$$\tilde{\underline{F}}_k = \tilde{\phi}(kT, (k-1)T) \quad (2.14)$$

$$\tilde{\underline{G}}_k = \int_0^T \tilde{\phi}(kT, \tau_1 + (k-1)T) \tilde{\underline{G}}_c(\tau_1 + (k-1)T) \tilde{\underline{\psi}}'(\tau_1) d\tau_1, \quad (2.15)$$

(2.13) becomes

$$\underline{\tilde{x}}_k = \tilde{\underline{F}}_k \underline{\tilde{x}}_{k-1} + \tilde{\underline{G}}_k \underline{u}_k \quad (2.16)$$

The output of the i^{th} data filter at $t = kT$, i.e., the i^{th} component of $\underline{\tilde{\ell}}_k$, is then

$$\begin{aligned} \tilde{\ell}_k^i &= \int_0^T \tilde{f}(\tau + (k-1)T) \tilde{g}_i(T - \tau) d\tau, \\ &= \int_0^T [\tilde{y}(\tau + (k-1)T) + \tilde{n}(\tau + (k-1)T)] \tilde{g}_i(T - \tau) d\tau. \end{aligned} \quad (2.17)$$

From (2.9) .

$$\begin{aligned} \tilde{\lambda}_k^1 &= \int_0^T \tilde{H}_c(\tau+(k-1)T) \tilde{x}(\tau+(k-1)T) \tilde{g}_1(T-\tau) d\tau \\ &+ \int_0^T \tilde{h}(\tau+(k-1)T) \tilde{g}_1(T-\tau) d\tau . \end{aligned} \quad (2.18)$$

The continuous time state equation (2.10) states that

$$\begin{aligned} \tilde{x}(\tau+(k-1)T) &= \tilde{\phi}(\tau+(k-1)T, (k-1)T) \tilde{x}(k-1)T \\ &+ \int_{(k-1)T}^{\tau+(k-1)T} \tilde{\phi}(\tau+(k-1)T, \tau_1) \tilde{G}_c(\tau_1) \tilde{u}(\tau_1) d\tau_1 . \end{aligned} \quad (2.19)$$

The change of variables

$$\tau_2 = \tau_1 - (k-1)T$$

applied to the integral in (2.19) produces

$$\begin{aligned} \tilde{x}(\tau+(k-1)T) &= \tilde{\phi}(\tau+(k-1)T, (k-1)T) \tilde{x}((k-1)T) \\ &+ \int_0^{\tau} \tilde{\phi}(\tau+(k-1)T, \tau_2+(k-1)T) \tilde{G}_c(\tau_2+(k-1)T) \tilde{u}(\tau_2+(k-1)T) d\tau_2 . \end{aligned} \quad (2.20)$$

Since

$$\tilde{u}(\tau_2+(k-1)T) = \tilde{\Phi}'(\tau_2) u_k , \quad 0 \leq \tau_2 \leq \tau \leq T, \quad (2.21)$$

(2.20) becomes

$$\tilde{\mathbf{x}}(\tau+(k-1)T) = \tilde{\Phi}(\tau+(k-1)T, (k-1)T)\tilde{\mathbf{x}}((k-1)T) \quad (2.22)$$

$$+ \int_0^T \tilde{\Phi}(\tau+(k-1)T, \tau_2+(k-1)T)\tilde{\mathbf{G}}_c(\tau_2+(k-1)T)\tilde{\Phi}'(\tau_2)\mathbf{u}_k, \quad 0 \leq \tau \leq T.$$

Equation (2.18) then becomes

$$\begin{aligned} \tilde{\mathbf{z}}_k^1 &= \int_0^T \tilde{\mathbf{H}}_c(\tau+(k-1)T)\tilde{\Phi}(\tau+(k-1)T, (k-1)T)\tilde{\mathbf{x}}((k-1)T)\tilde{\mathbf{g}}_1(T-\tau)d\tau \\ &+ \int_0^T \tilde{\mathbf{H}}_c(\tau+(k-1)T)\left[\int_0^T \tilde{\Phi}(\tau+(k-1)T, \tau_2+(k-1)T)\tilde{\mathbf{G}}_c(\tau_2+(k-1)T)\right. \\ &\times \tilde{\Phi}'(\tau_2)\mathbf{u}_k\tilde{\mathbf{g}}_1(T-\tau)d\tau_2 + \int_0^T \tilde{\mathbf{n}}(\tau+(k-1)T)\tilde{\mathbf{g}}_1(T-\tau)d\tau \end{aligned} \quad (2.23)$$

Define two observation matrices $\tilde{\mathbf{H}}_k^1$ and $\tilde{\mathbf{H}}_k^2$ such that

$$\text{the } i^{\text{th}} \text{ row of } \tilde{\mathbf{H}}_k^1 = \int_0^T \tilde{\mathbf{H}}_c(\tau+(k-1)T)\tilde{\Phi}(\tau+(k-1)T, (k-1)T)\tilde{\mathbf{g}}_1(T-\tau)d\tau, \quad (2.24)$$

$$i = 1, \dots, N_f,$$

and

$$\begin{aligned} \text{the } i^{\text{th}} \text{ row of } \tilde{\mathbf{H}}_k^2 &= \int_0^T \tilde{\mathbf{H}}_c(\tau+(k-1)T)\tilde{\mathbf{g}}_1(T-\tau)\left[\int_0^T \tilde{\Phi}(\tau+(k-1)T, \tau_2+(k-1)T)\right. \\ &\times \tilde{\mathbf{G}}_c(\tau_2+(k-1)T)\tilde{\Phi}'(\tau_2)\mathbf{u}_k\tilde{\mathbf{g}}_1(T-\tau)d\tau_2 \left. + \int_0^T \tilde{\mathbf{n}}(\tau+(k-1)T)\tilde{\mathbf{g}}_1(T-\tau)d\tau \right] d\tau, \quad i = 1, \dots, N_f. \end{aligned} \quad (2.25)$$

Also, define a discrete time noise vector $\tilde{\mathbf{n}}_k$ whose i^{th} component is

$$\tilde{n}_k^i = \int_0^T \tilde{\mathbf{n}}(\tau+(k-1)T)\tilde{\mathbf{g}}_1(\tau)d\tau, \quad i = 1, \dots, N_f. \quad (2.26)$$

The noise statistics are then

$$E[\tilde{\mathbf{n}}_1] = \mathbf{0}, \quad (2.27)$$

$$K_{ij} = E[\tilde{\mathbf{n}}_i \tilde{\mathbf{n}}_j^\dagger] = N_0 \int_0^T \tilde{g}_i(\tau) \tilde{g}_j^*(\tau) d\tau, \quad (2.28)$$

where

$$\mathbf{x}^\dagger = (\mathbf{x}^*)',$$

and

$$E[\tilde{\mathbf{n}}_i \tilde{\mathbf{n}}_j'] = 0. \quad (2.29)$$

Insertion of the defined parameters into (2.23) produces the expression for the vector of statistics,

$$\tilde{\mathbf{z}}_k = \tilde{\mathbf{H}}_k^1 \tilde{\mathbf{x}}_{k-1} + \tilde{\mathbf{H}}_k^2 \mathbf{u}_k + \tilde{\mathbf{n}}_k. \quad (2.30)$$

Derivation of the Equations for FDIR Channels

A set of discrete time equations, having the same form as those developed previously for state variable model channels, (2.16) and (2.30), is developed in this section for FDIR channel models. The state of an FDIR channel is defined to be the $(L \times M) \times 1$ vector \mathbf{x}_k , which in partitioned form is

$$\mathbf{x}_k = \begin{bmatrix} \mathbf{u}_k \\ \mathbf{u}_{k-1} \\ \vdots \\ \mathbf{u}_{k-L+1} \end{bmatrix}. \quad (2.31)$$

The submatrices are the present symbol and the previous $L-1$ symbols, where LT is the length of the zero state response of the channel to a single pulse.

The continuous time output of the channel filter is given by

$$\tilde{y}(t) = \int_0^t \tilde{h}(t, \tau) \tilde{u}(\tau) d\tau. \quad (2.32)$$

Substituting (2.1) into the above and using the FDIR assumption,

$$\tilde{y}(t) = \int_0^t \tilde{h}(t, \tau) \sum_{j=k-L+1}^k \tilde{\Phi}'(\tau - (j-1)T) d\tau \underline{u}_j, \quad (k-L)T < t < kT \quad (2.33)$$

is obtained. Interchanging integration and summation,

$$\tilde{y}(t) = \sum_{j=k-L+1}^k \int_0^t \tilde{h}(t, \tau) \tilde{\Phi}'(\tau - (j-1)T) d\tau \underline{u}_j, \quad (k-L)T < t < kT \quad (2.34)$$

$$= \sum_{j=k-L+1}^k \tilde{y}_j'(t) \underline{u}_j, \quad (k-L)T < t < kT, \quad (2.35)$$

where

$$\tilde{y}_j(t) = \int_0^t \tilde{h}(t, \tau) \tilde{\Phi}(\tau - (j-1)T) d\tau. \quad (2.36)$$

The set of $M \times 1$ vectors,

$$\left\{ \tilde{y}_j(t + (n-1)T) \right\}_{n=1}^L, \quad (2.37)$$

represent the L vector "chips" of the zero state response of the channel to $\tilde{\Phi}(t)$.

Each filter in the bank of matched filters has an impulse response which is related to the chip by

$$\tilde{g}_j(t) = \tilde{y}_j^*(T-t), \quad 0 < t < T. \quad (2.38)$$

The output of the i^{th} filter can be written,

$$\tilde{z}_k^i = \int_0^T \tilde{g}_i(T-\tau) \sum_{j=k-L+1}^k \tilde{y}_j'(\tau) d\tau \underline{u}_j + \int_0^T \tilde{g}_i(T-\tau) \tilde{n}(\tau) d\tau, \quad (2.39)$$

$$i = 1, \dots, L.$$

Substituting (2.38) into (2.39),

$$\tilde{z}_k^i = \int_0^T \tilde{y}_i^*(\tau) \sum_{j=k-L+1}^k \tilde{y}_j'(\tau) d\tau \underline{u}_j + \int_0^T \tilde{y}_i^*(\tau) \tilde{n}(\tau) d\tau, \quad (2.40)$$

$$i = 1, \dots, L.$$

Interchanging integration and summation in the first term of (2.40),

$$\tilde{z}_k^i = \sum_{j=k-L+1}^k \int_0^T \tilde{y}_i^*(\tau) \tilde{y}_j'(\tau) d\tau \underline{u}_j + \int_0^T \tilde{y}_i^*(\tau) \tilde{n}(\tau) d\tau, \quad (2.41)$$

$$i = 1, \dots, L.$$

Breaking out the k^{th} term of the summation,

$$\begin{aligned} \tilde{\underline{\ell}}_k^1 = & \sum_{j=k-L+1}^{k-1} \int_0^T \tilde{\underline{y}}_i^*(\tau) \tilde{\underline{y}}_j'(\tau) d\tau \underline{u}_j + \int_0^T \tilde{\underline{y}}_i^*(\tau) \tilde{\underline{y}}_k'(\tau) d\tau \underline{u}_k \\ & + \int_0^T \tilde{\underline{y}}_i^*(\tau) \tilde{n}(\tau) d\tau, \quad i = 1, \dots, L. \end{aligned} \quad (2.42)$$

This set of equations can be written as

$$\tilde{\underline{\ell}}_k^1 = \tilde{H}_1^1 \underline{x}_{k-1} + \tilde{H}_2^1 \underline{u}_k + \tilde{\underline{n}}_k^1, \quad i = 1, \dots, L, \quad (2.43)$$

where

$$\tilde{H}_1^1 = \begin{bmatrix} \tilde{H}_1^{1,1} & \tilde{H}_1^{1,2} & \dots & \tilde{H}_1^{1,L-1} & 0 \end{bmatrix}, \quad (M \times (M \times L)), \quad (2.44)$$

$$\tilde{H}_1^{1,j} = \int_0^T \tilde{\underline{y}}_i^*(\tau) \tilde{\underline{y}}_j'(\tau) d\tau, \quad i = 1, \dots, L, \quad j = 1, \dots, L-1, \quad (2.45)$$

$$\tilde{H}_2^1 = \int_0^T \tilde{\underline{y}}_i^*(\tau) \tilde{\underline{y}}_k'(\tau) d\tau, \quad i = 1, \dots, L, \quad (2.46)$$

$$\tilde{\underline{n}}_k^1 = \int_0^T \tilde{\underline{y}}_i^*(\tau) \tilde{n}(\tau) d\tau, \quad i = 1, \dots, L. \quad (2.47)$$

The noise statistics are given by

$$E[\tilde{\underline{n}}_k^i] \equiv \underline{0}, \quad (2.48)$$

$$K_{ij} = E[\tilde{\underline{n}}_k^i \tilde{\underline{n}}_k^{j\dagger}] = N_0 \int_0^T \tilde{\underline{g}}_i(\tau) \tilde{\underline{g}}_j^\dagger(\tau) d\tau, \quad (2.49)$$

and

$$E[\tilde{\underline{n}}_k^i \tilde{\underline{n}}_k^j] \equiv 0. \quad (2.50)$$

The recursive equations are then

$$\underline{x}_k = \begin{bmatrix} 0 & 0 \\ \vdots & \vdots \\ \underline{I}_M \times (L-1) & 0 \end{bmatrix} \underline{x}_{k-1} + \begin{bmatrix} \underline{u}_k \\ 0 \\ \vdots \\ 0 \end{bmatrix}, \quad (2.51)$$

$$\tilde{\underline{g}}_k^i = \tilde{H}_1^i \underline{x}_{k-1} + \tilde{H}_2^i \underline{u}_k + \tilde{\underline{n}}_k^i, \quad i = 1, \dots, L. \quad (2.43)$$

CHAPTER III

DEVELOPMENT OF THE ESTIMATE FEEDBACK DETECTOR

Introduction

In this chapter the suboptimum detector developed in this research is defined. First the optimum detector is specified.

The optimum detector is defined here to be the detector with minimum probability of symbol error. This detector generates the posterior probabilities

$$p(\underline{u}_k = \underline{A}_i | r(t), \quad 0 < t < (k+D)T), \quad i = 1, \dots, M, \quad (3.1)$$

and if the j^{th} probability is the largest of the set, the decision is

$$d(\underline{u}_k) = \underline{A}_j. \quad (3.2)$$

D is a parameter that represents the ability of the detector to delay the decision for D signaling intervals after the onset of energy from the k^{th} pulse.

As shown in [23], for the WGN case with no channel memory, it is possible to substitute conditional dependency on a sequence of sufficient statistic vectors,

$$L_{k+D} = \{\tilde{l}_j\}_{j=1}^{k+D}, \quad (3.3)$$

for conditional dependency on the waveform $r(t)$ over $[0, (k+D)T]$. A similar derivation for the channel models considered here of sufficient statistics in Appendix A shows that a set of sufficient statistics is generated as the sampled outputs of a bank of N matched filters. For example, consider the case of a time-invariant state channel model whose frequency response is properly symmetric (amplitude response even and phase response odd about f_c) and in which the modulation is BPSK. The number of required matched filters is $N = N_h + 1 - N_h$ filters matched to the N_h homogeneous solutions of the state equation and one matched to the forced response of the channel.

For the FDIR channel model case, a set of L matched filters, where L is the length of the zero state response, will generate a vector of sufficient statistics for the detector. Each filter is matched to a chip of the zero state response [16]. Next, various detector algorithms are discussed.

Development of the Estimate Feedback Detector for FDIR Channels

The optimum detection algorithm for FDIR channels, assuming a delay D and a channel response to a single signaling pulse of integer length L , was developed by Abend and Fritchman [15]. They obtained a recursive algorithm for generating the posterior sequence probability,

$$P(u_{k+D-L+1}, u_{k+1}, \dots, u_{k+D} | L_{k+D}) . \quad (3.4)$$

To generate this density a dynamic model for the channel memory is required. In the FDIR case a discrete convolution is used in the algorithm

to generate these sequence probabilities.

The decision is then made based on the \underline{A}_i that maximizes

$$p(\underline{u}_k = \underline{A}_i | L_{k+D}) . \quad (3.5)$$

For the case of most interest, in which $D \leq L-1$,

$$p(\underline{u}_k = \underline{A}_i | L_{k+D}) = \text{const} \quad (3.6)$$

$$\times \left(\sum_{\underline{u}_{k+D-L+1}} \cdots \sum_{\underline{u}_{k-1}} \sum_{\underline{u}_{k+1}} \cdots \sum_{\underline{u}_{k+D}} p(\underline{u}_{k+D-L+1} \cdots \underline{u}_{k+D} | L_{k+D}) \right)$$

In general one would like to keep D as small as possible. With the Abend-Fritchman (A-F) algorithm, however, $M^{\max\{L, D+1\}}$ probabilities must be generated after every signaling interval. In a real situation L could be 10 or larger so that the algorithm can be computationally complex even when D is chosen to be small.

A reasonable approach to reducing the complexity of the A-F algorithm is to use an estimate of the symbol \underline{u}_{k-1} as if it were the correct symbol and thus only the probabilities (M^{D+1} in number) corresponding to all possible combinations of sequences,

$$\{\underline{u}_k, \underline{u}_{k+1}, \cdots, \underline{u}_{k+D}\} , \quad (3.7)$$

are needed.

A number of ways of generating such an estimate exist. In a hard

decision-directed (HDD) approach, all previous decisions are assumed to be correct, and the algorithm for the decision on u_k is computed based on the hypothesis that

$$\hat{u}_{k-1} = d(u_{k-1}) , \quad (3.8)$$

where the carat denotes an estimate and the function d is the decision function. This philosophy is used in [10,11]. For large SNR this detector works well, but it is marginally effective at lower SNR because errors tend to avalanche [10]. This detector, however, is less complex than most other suboptimum detectors. The canonic HDD structure is shown in Figure 3.

In Figure 4 the soft decision-directed (SDD) canonic form is shown. Here the detector output (in the binary antipodal signaling over a carrier symmetric channel case) is passed through an NLNM device such as one whose characteristic is a soft limiter or a hyperbolic tangent [12,13].

If one of the posterior probabilities is close to one, essentially a hard decision is made. If no probability is close to one, the estimate is a number between (-1) and $(+1)$ -- i.e., a hedged decision. Better results are obtained by using an SDD approach than by taking an HDD approach, particularly at low SNR [12].

The approach put forward here is to use the basic A-F algorithm but to reduce its complexity by combining the posterior probabilities into an estimate of u_{k-1} ,

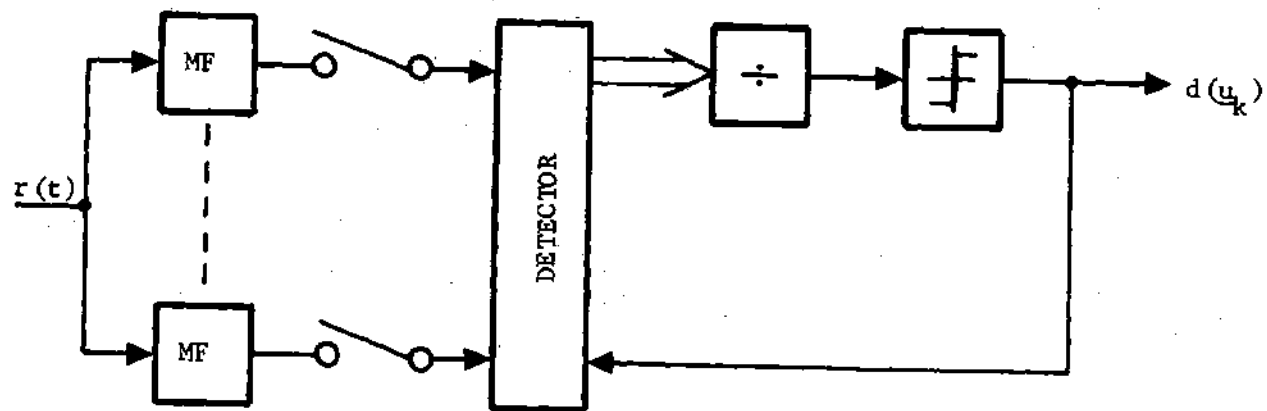


Figure 3. Hard Decision Directed Binary Detector for FDIR Channels

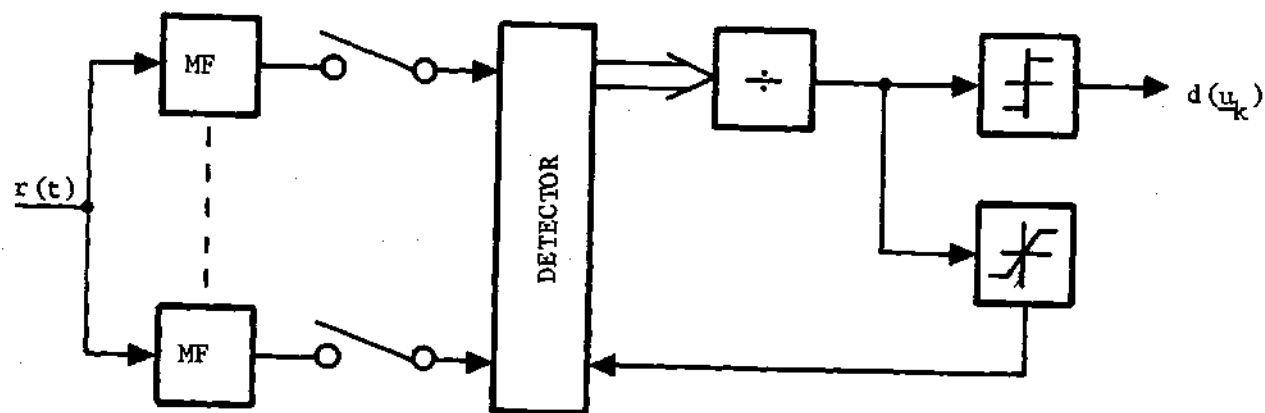


Figure 4. Soft Decision Directed Binary Detector for FDIR Channels

$$\hat{u}_{k-1} = \hat{E}\{u_{k-1} | L_{k+D}\}, \quad (3.9)$$

or

$$\hat{u}_{k-1} = \sum_{i=1}^M \frac{A_i}{M} \hat{p}(u_{k-1} = A_i | L_{k+D-1}).$$

Of course, it would be nice to have the exact posterior probabilities, but these are not available from a suboptimum algorithm. Nonetheless this detector has a number of desirable properties:

1. It is computationally simpler than the A-F algorithm in that the number of sequences considered is M^D rather than M^L when $D < L-1$.
2. The posterior probabilities needed for the calculation of the estimate are already being generated as part of the detection algorithm.
3. The detector is theoretically optimum in the limit as D increases. Therefore, the way to modify the detector for better performance and the cost in complexity to get that performance are clear.

In summary, for FDIR channel models, the estimate feedback detector uses the basic A-F algorithm but reduces complexity by shortening the sequence lengths and adjusting for the loss in performance with feedback of approximate MAP estimates of symbols that are no longer a part of the sequence. The general canonic structure of this detector is shown in Figure 5. The estimate feedback algorithm is given in Appendix C.

Development of the Estimate Feedback Detector for State Variable Channels

In this section the estimate feedback detector developed previously for FDIR channel models is applied to state variable channel models. The motivation is the desire to develop a detector that could be implemented

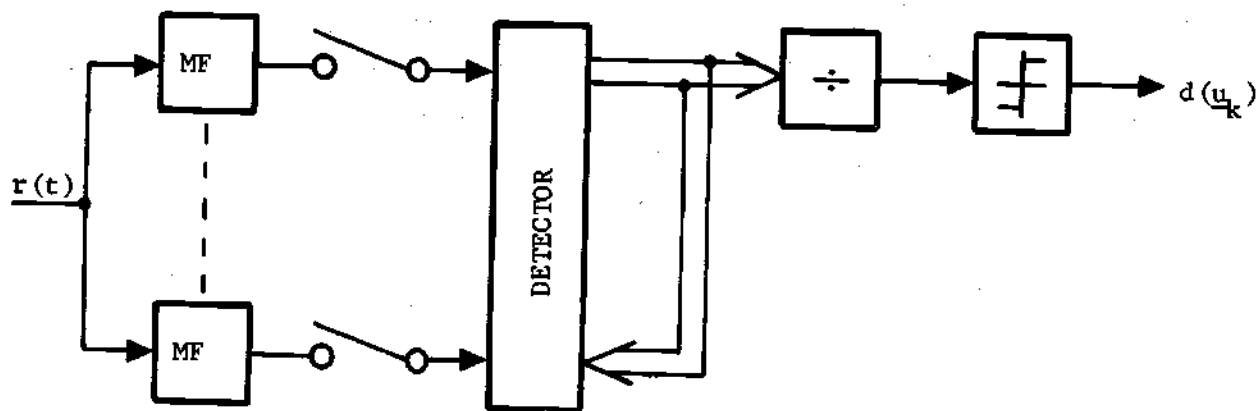


Figure 5. Estimate Feedback Binary Detector for FDIR Channels

by using estimates of the channel state to reduce computational complexity.

Assume that the filter portion of the channel can be modeled by the state equation developed in Chapter II,

$$\tilde{\mathbf{x}}_k = \tilde{\mathbf{F}}_k \tilde{\mathbf{x}}_{k-1} + \tilde{\mathbf{G}}_k u_k, \quad (3.10)$$

and that the observation vector (each component being the sampled output of one of the filters in the bank of matched filters) can be written

$$\tilde{\mathbf{z}}_k = \tilde{\mathbf{H}}_k^1 \tilde{\mathbf{x}}_{k-1} + \tilde{\mathbf{H}}_k u_k + \tilde{\mathbf{n}}_k. \quad (3.11)$$

Consider the case where $D = 0$. It can be seen from the state equation that if the state of the channel filter, $\tilde{\mathbf{x}}_{k-1}$, is known at the beginning of a signaling interval, the channel output caused by all previous symbols can be subtracted out. In other words the intersymbol interference problem would reduce to the simple detection problem of testing between M known signals with observation,

$$\tilde{\mathbf{z}}_k = \tilde{\mathbf{H}}_k^2 u_k + \tilde{\mathbf{n}}_k', \quad (3.12)$$

where $\tilde{\mathbf{n}}_k$ is Gaussian with known mean $\tilde{\mathbf{H}}_k^1 \tilde{\mathbf{x}}_{k-1}$.

For $D > 0$ it is appropriate to generate an estimate of the state of the channel D signaling intervals behind the incoming data. The sequence length, $D+1$, of the detector algorithm can be kept small without severe performance degradation if a reasonably good state estimate is employed.

In developing a suboptimum detection algorithm employing a state estimate, a number of approaches are possible. In an HDD approach, the detector output is assumed to be correct, and the algorithm for the decision on \underline{u}_k is generated based on the hypothesis that

$$\hat{\underline{x}}_{k-1} = \tilde{F}_{k-1} \hat{\underline{x}}_{k-2} + \tilde{G}_{k-1} d(\underline{u}_{k-1}) . \quad (3.13)$$

The functional block diagram for this case is shown in Figure 6. The case of $D = 0$ was treated in [11].

In Figure 7 the SDD canonic structure is shown. In a manner similar to that for an FDIR channel model, the detector output is passed through an NLNM device, then through a state model representing the channel memory.

The optimum Bayes estimate of the state of a system at time k , given observations up to and including $\tilde{\underline{y}}_{k+D}$ is given by

$$\hat{\underline{x}}_k = \sum_{j=1}^{M^{k+D}} P(\underline{u}_k = \underline{A}_j | L_{k+D}) E[\tilde{\underline{x}}_k | \underline{u}_k = \underline{A}_j, L_{k+D}] . \quad (3.14)$$

Here, each of the expected values represents a special case of a Kalman smoothing estimator for the problem in which the first order density of the system excitation process is given by a linear combination of M Gaussian densities, i.e., a mixture, but in which each density has zero variance.

Ackerson and Fu [24] first developed the least squares estimate for the $D = 0$ case and also considered a suboptimum estimator. They

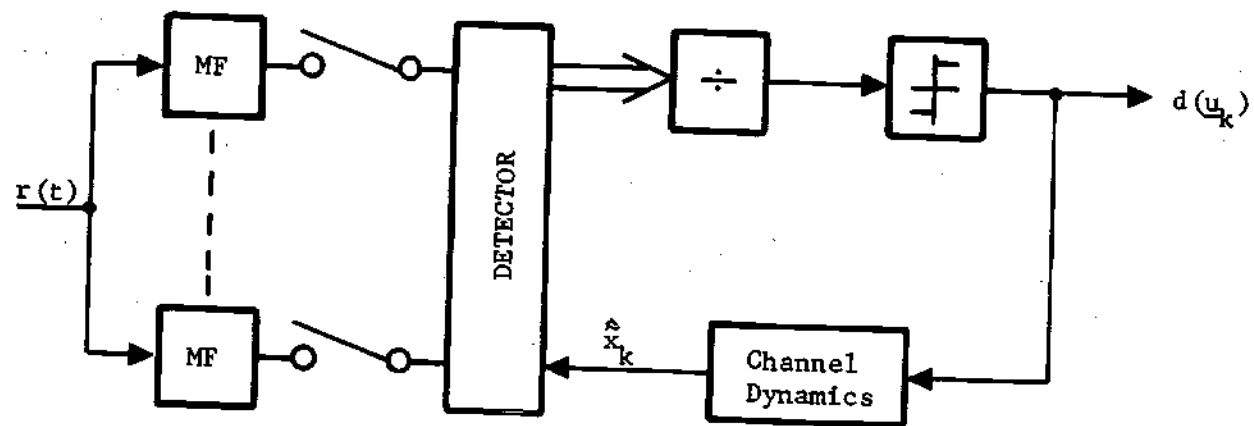


Figure 6. Hard Decision Directed Binary Detector for State Variable Channels

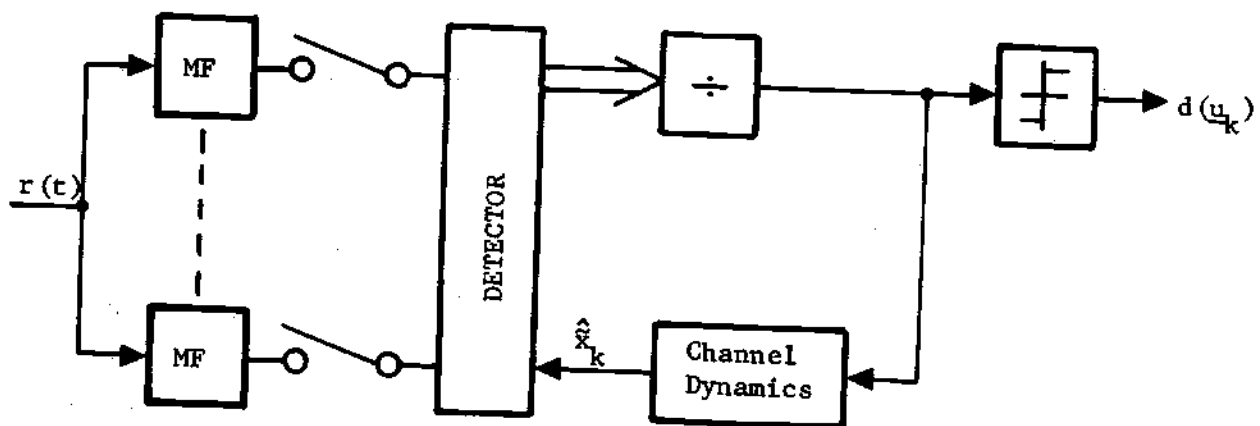


Figure 7. Soft Decision Directed Binary Detector for State Variable Channels

applied their results to a controls application, but their work provided the original motivation for this research into a possible digital communications application. It soon became apparent that to extend their approach to the realizable-with-delay case ($D > 0$) would lead to a quite complex fixed lag smoothing algorithm and would thus not be profitable.

The basis for this research is to feed back posterior probabilities in a Bayesian type of estimate rather than the information lossy HDD approach or an ad hoc SDD approach. Figure 8 shows the canonic structure of the detector developed in this report.

The A-F algorithm can be applied directly to channels with state variable models. The basic A-F algorithm generates M^L estimates of what the observation should look like conditioned on a particular input sequence. It then compares the conditional estimates with the actual observation and generates M^L posterior sequence probabilities. A dynamic model of the channel memory must be a part of the detector algorithm in order to generate an output from a conditional set of inputs. In Abend and Fritchman's original work [15], a sampled data model for the channel output was assumed (the FDIR assumption), and outputs were calculated by discrete convolution.

In Chapter II a recursive state and observation equation pair was derived from the discrete convolution model of channel dynamics. The state and observation equations could thus be used in the A-F algorithm. Also, in Chapter II, a pair of state and observation equations was derived under the assumption of a continuous time state model channel. The form and function of these equations were identical to the set of equations derived under the FDIR assumption. Consequently they could be

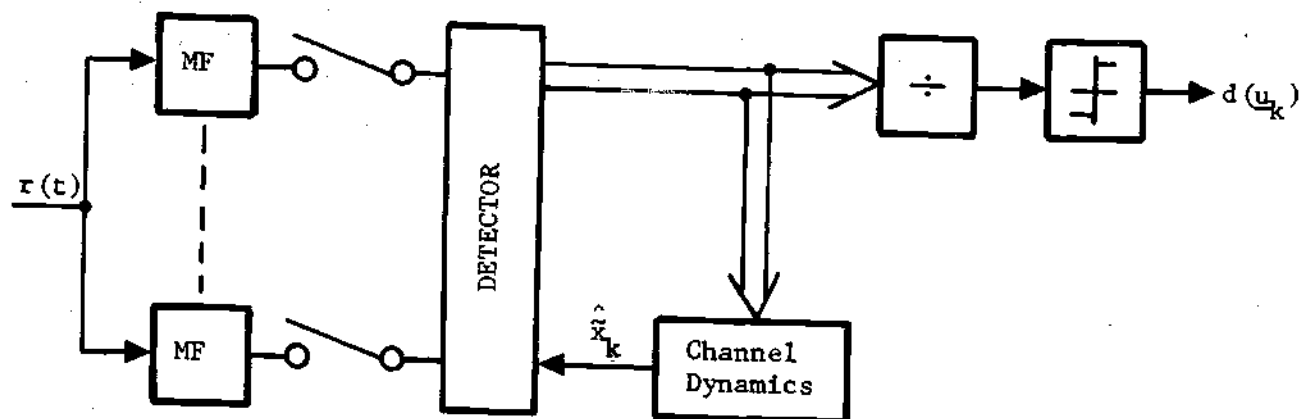


Figure 8. Estimate Feedback Binary Detector for State Variable Channels

incorporated into the A-F algorithm as the dynamic model.

Since the estimate feedback detector uses a channel model for the same purpose as does the A-F detector, i.e., to generate outputs based on conditional input sequences, it can likewise use either channel model. The channel state estimate is produced by calculating a symbol estimate by

$$\hat{u}_{k-1} = \sum_{i=1}^M \frac{A_i}{\sum_{j=1}^M A_j} \hat{p}(u_{k-1} = A_i | L_{k+D-1}) , \quad (3.15)$$

and driving a recursive state model with the sequence of symbol estimates. Thus the estimate feedback detector can be used with state variable channel models. The estimate feedback algorithm is given in Appendix C.

Comparison of the A-F Detector with the Viterbi Detector

The Viterbi algorithm (VA) can also be used as a detector for dispersive channels [16]. If delay is infinite, it is optimum but for finite fixed delay D it is suboptimum just as the A-F and estimate feedback detectors are. Other disadvantages are that:

1. it has been applied only to FDIR channel models, and it uses sequences of length L just as the A-F detector does.
2. to modify it for minimum symbol errors rather than sequence errors considerably increases complexity [28].
3. there is no simple relationship between the state metric and the quality of the detection [28] for the VA as there is with A-F or estimate feedback detection.

An Error Rate Estimate

It is important in many operational situations to have a performance monitor that indicates the status of the link. Such an indication in present day systems has usually come from a channel error decoder or perhaps from a frame synchronizer in the receiver.

When detectors that generate fairly accurate posterior probabilities are used, an estimate of the error rate is presented here that from the simulation results appears to be quite accurate. Consider the binary case. The estimate is based on the expression for symbol error rate derived in Appendix B. Equation (B1.10) states that for any detector,

$$p_e = E_{L_{k+D}} \left[\min_1 p(u_k = \underline{A}_1 | L_{k+D}) \right] . \quad (3.16)$$

The estimate for error probability is

$$\hat{p}_e^k = \frac{1}{k} \sum_{j=1}^k \min_1 \hat{p}(u_j = \underline{A}_1 | L_{j+D}) , \quad (3.17)$$

namely the sample mean of the smaller of the two posterior symbol probabilities. This estimate should converge in the m.s. sense to p_e as $k \rightarrow \infty$ if

$$\sigma_{\hat{p}_e^k} \rightarrow 0 \quad (3.18)$$

as $k \rightarrow \infty$ according to the Markoff law of large numbers [27]. However this appears impossible to ascertain because of the complexity of (3.17). Simulation results for this binary case are presented in Chapter IV.

CHAPTER IV

RESULTS OF THE COMPUTER SIMULATIONS

Introduction

The purpose of this chapter is to present the computer simulation results for the detector algorithm developed here and for a number of other detectors found in the literature. Exact analytical results for error rate have not been obtained for this problem although approximate results and upper and lower bounds have been determined in some cases; e.g., [11,16]. Since Monte Carlo simulations give an accurate indication of performance for specific cases, they were used to generate comparisons among the various detectors.

Three specific channels were simulated to determine results of this detector algorithm. Each was a WGN channel with channel filtering modeled as

1. a one pole Butterworth state variable model with $T = 1$ and $\omega_c = 1$,
2. a two pole Butterworth state variable model with $T = 1$ and $\omega_c = \pi$,
3. an FDIR model, used by Abend and Fritchman [15], representing a channel response measured on a Bell System data line; the sampled channel response is $(-0.077, -0.355, 0.059, 1.000, 0.059, -0.273)$.

Binary PSK signaling with NRZ pulses is used in all simulations.

The energy in the channel response is defined to be that over $[0, \infty)$. In each case a set of discrete time equations representing the evolution of the state of the channel filter and of the observation is developed. The input to the recursion is a sequence of symbols and the output is a sequence of observations L_k .

In the state variable model case the observations are the sampled outputs of a bank of filters, derived in Appendix A, which are a set of sufficient statistics for this problem. In the FDIR case, the recursion output is selected to be the sequence of samples of the channel output (no filtering) so as to agree with Abend and Fritchman [15].

A uniform pseudo random number generator is used to generate the data sequence, and a Gaussian pseudo random number generator is used to generate the WGN. A number of statistical tests and histograms were run on different generators to obtain a good generation algorithm and to determine good starting numbers. For the case in which a bank of filters is used, the noise portions of the filter outputs are correlated for a given k , and a linear transformation of a vector of independent Gaussian variables is necessary to obtain the proper correlation.

The detector is initialized so that the errors counted are steady state errors. For example, in simulating the $D = 2$ detector, the detector for $D = 0$ is first used. It combines two prior probabilities of 0.5 with \tilde{L}_1 and produces two posterior probabilities. Next the $D = 1$ detector is used. The four prior probabilities it requires, one for each possible sequence of u_1 and u_2 , are generated from the two posterior probabilities produced by the $D = 0$ detector. The $D = 1$ detector combines these four

priors with $\tilde{\ell}_2$ and generates a set of four posterior sequence probabilities. In a similar manner these four probabilities are transformed into eight priors that are combined with $\tilde{\ell}_3$ by a $D = 2$ detector to yield a set of eight posterior sequence probabilities. The $D = 2$ detector is used exclusively from this point on in the recursion. It takes the eight posterior sequence probabilities, combines them with $\tilde{\ell}_4$, and produces eight posterior sequence probabilities that may be assumed suitable for error count. The eight posterior sequence probabilities are combined so that all probabilities with a (-1) in the $k = 1$ position are added together and those with a (+1) are added together. This produces the two posterior symbol probabilities from which a decision about the $k = 1$ symbol is made. The decision is compared with the actual symbol used to generate the observations, and an error count is kept.

It is obvious from the above that the detector algorithm could be stopped after the calculation of the posterior sequence probabilities and the decision made based on the largest posterior sequence probability. This points out the fact that the detector developed here could also be used in a minimum sequence error mode if so desired to save complexity.

All results shown were obtained by actual simulation using the same pseudo random number sequences. No results generated from different sequences of PN numbers were copied from the literature so that as accurate a comparison as possible is obtained.

Presentation of Monte Carlo Results

Figure 9 shows the simulation results for a one pole Butterworth filter channel. The vector of sufficient statistics is generated by correlating the input waveform with the two time functions,

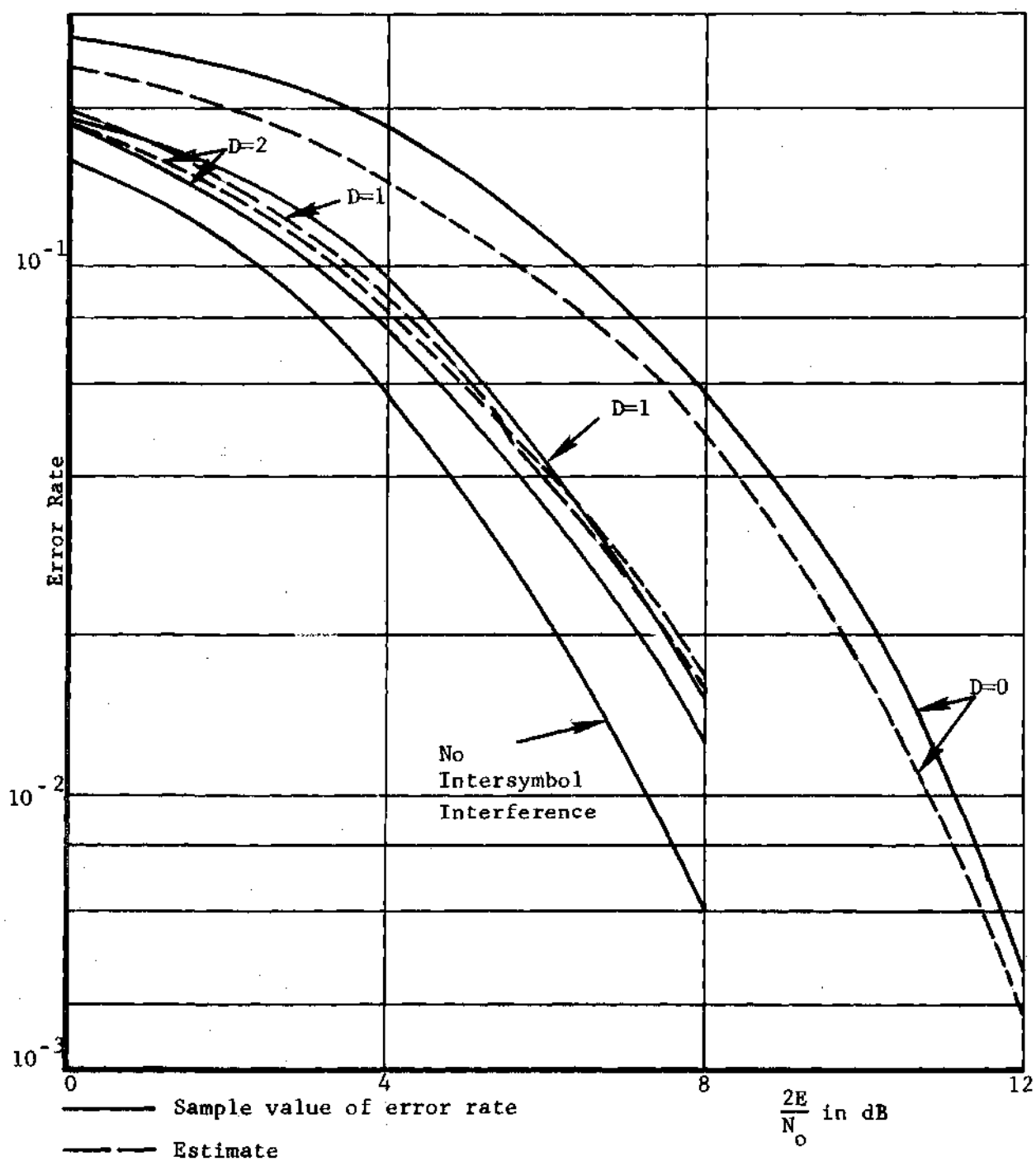


Figure 9. Error Rate of a One Pole Butterworth Filter
with $f_{co} = 1/2\pi$ and $T = 1$

$$g_1(t) = C_1(1 - e^{-pt}) , \quad 0 < t < T, \quad (4.1a)$$

$$g_2(t) = C_2 e^{-pt} , \quad 0 < t < T, \quad (4.1b)$$

where p is the pole location of the channel filter, and C_1, C_2 are normalization constants. The filters are sampled and dumped every T seconds.

The state and observation equations for this example with $p = 1$, $T = 1$, are,

$$x_k = 0.368 x_{k-1} + 0.632 \sqrt{E} u_k \quad (4.2a)$$

$$\underline{z}_k = \begin{bmatrix} 0.487 \\ 0.658 \end{bmatrix} x_{k-1} + \begin{bmatrix} 1.000 \\ 0.741 \end{bmatrix} \sqrt{E} u_k + \underline{n}_k . \quad (4.2b)$$

The correlation matrix of the observation noise \underline{n}_k is

$$R = \begin{bmatrix} 1.000 & 0.741 \\ 0.741 & 1.000 \end{bmatrix} . \quad (4.2c)$$

The error rate estimate shown in Figure 9 and all following error rate performance curves are obtained using the estimate discussed at the end of Chapter III, namely

$$\hat{p}_e = \frac{1}{k} \sum_{j=1}^k \min_i [\hat{p}(u_k = A_j | L_{j+D})] . \quad (4.3)$$

The error rate monitor approximates the expected value, over all L_{k+D} , by a sample mean. In addition it uses approximately correct posterior symbol probabilities.

One can see from the results how the error rate decreases as D is increased. It is also clear that the error rate estimate tracks the Monte Carlo results with good accuracy.

In Figure 10 the simulation results for the two pole Butterworth filter are shown. The sufficient statistics in this example are generated by correlating $r(t)$ with the three waveforms,

$$g_1(t) = C_1 \left(1 - e^{-\frac{\omega_c}{2} t} \left(\cos \frac{\omega_c}{2} t + \sin \frac{\omega_c}{2} t \right) \right), \quad 0 < t < T,$$

$$g_2(t) = C_2 e^{-\frac{\omega_c}{2} t} \left(\cos \frac{\omega_c}{2} t + \sin \frac{\omega_c}{2} t \right), \quad 0 < t < T,$$

$$g_3(t) = C_3 e^{-\frac{\omega_c}{2} t} \sin \frac{\omega_c}{2} t, \quad 0 < t < T,$$

where ω_c is the radian cutoff frequency and C_1, C_2, C_3 are normalization constants. The filters are sampled and dumped every T seconds.

The state and observation equations for this example with $\omega_c = 1$, $T = 1$, are,

$$\underline{x}_k = \begin{bmatrix} 0.021 & 0.039 \\ -0.383 & -0.152 \end{bmatrix} \underline{x}_{k-1} + \begin{bmatrix} 0.980 \\ 0.383 \end{bmatrix} \sqrt{E} u_k \quad (4.4a)$$

$$\underline{l}_k = \begin{bmatrix} 0.233 & 0.079 \\ 0.580 & 0.087 \\ 0.478 & 0.106 \end{bmatrix} \underline{x}_{k-1} + \begin{bmatrix} 0.614 \\ 0.247 \\ 0.459 \end{bmatrix} \sqrt{E} u_k + \underline{n}_k. \quad (4.4b)$$

The correlation matrix of the observation noise \underline{n}_k is

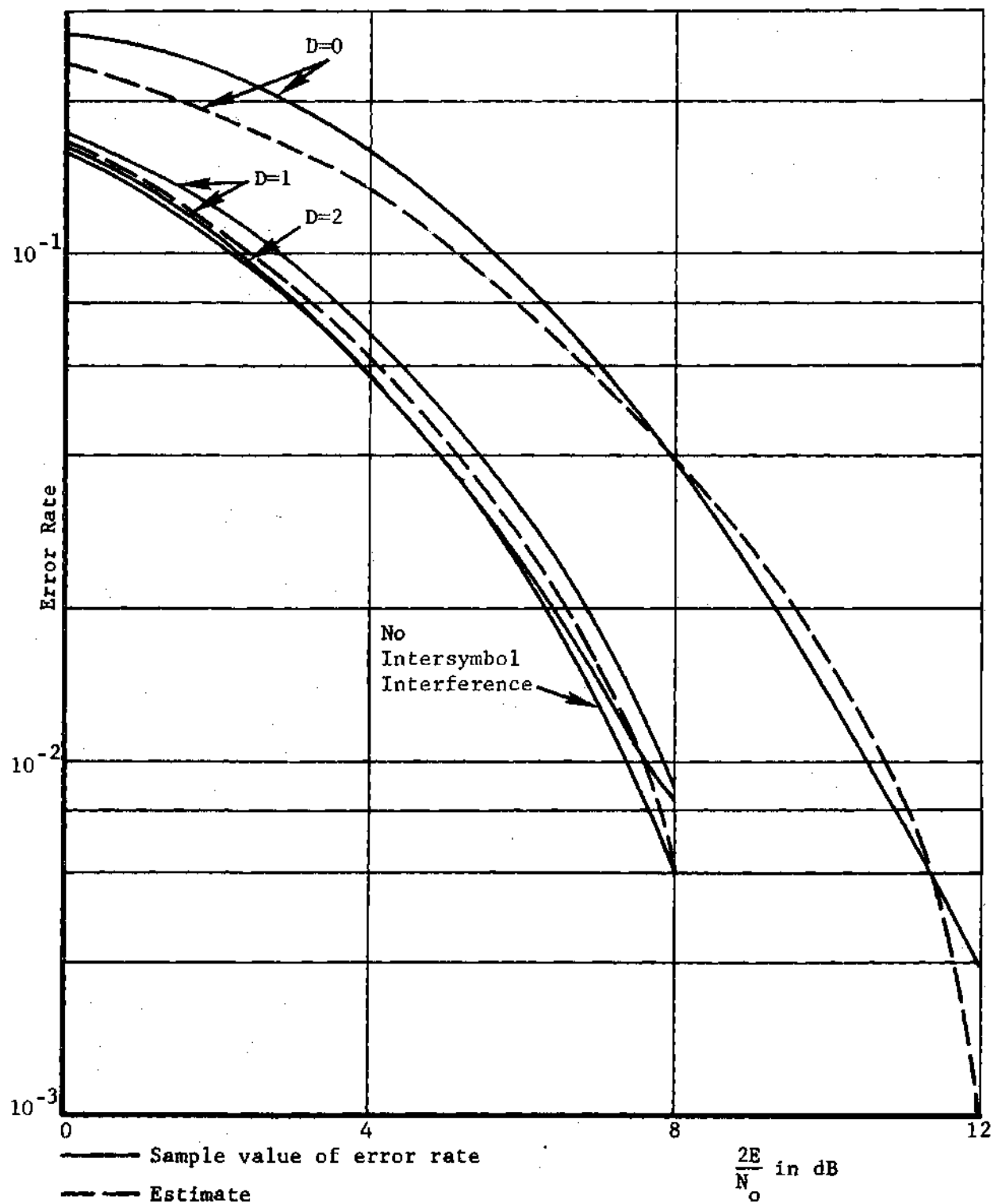


Figure 10. Error Rate of a Two Pole Butterworth Filter
with $f_{co} = .5$ and $T = 1$

$$R = \begin{bmatrix} 1.000 & 0.402 & 0.747 \\ 0.402 & 1.000 & 0.824 \\ 0.747 & 0.824 & 1.000 \end{bmatrix} . \quad (4.4c)$$

Once again the benefit in performance gained by delaying a decision is evident. The performance of the detector is effectively optimum for $D = 2$. Also, the error rate estimate demonstrates excellent results.

The detector developed here is also applicable to FDIR model channels. Figures 11 through 16 present the results of applying this detector to the Bell data line model and comparing the results with those obtained with the A-F detector. It should be noted that their detector is more complicated than the one developed here in all cases where $D < L-1$. This is because the A-F detector always generates 2^L sequence probabilities while the estimate feedback detector generates 2^{D+1} sequence probabilities.

In the figures the error rate and the error rate estimate for the estimate feedback detector are compared with results using the A-F detector and with the error rate estimate using the A-F posterior symbol probabilities. Results are shown sequentially for values of D from zero to five. Note that for $D \geq 3$ the estimate feedback detector performs as well as the A-F detector. For $D = 3$, the A-F detector generates four times as many sequence probabilities as the estimate feedback detector.

Figures 17 and 18 present a comparison between six different detectors for the one and two pole channel models, respectively. Results are shown for the following detectors:

1. a detector which thresholds the sampled output of a filter matched to the signaling pulse (an NRZ pulse in this case),

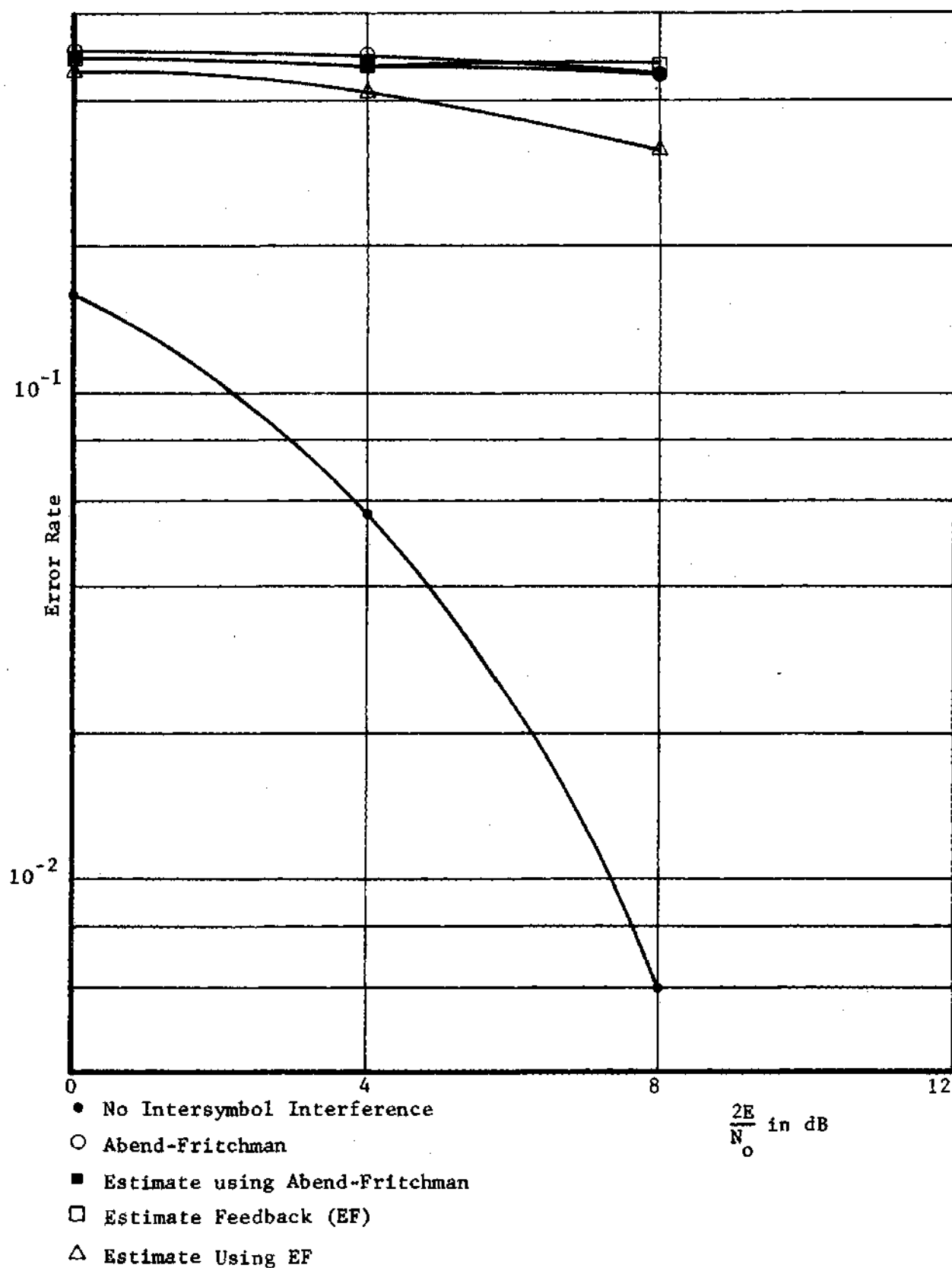


Figure 11. Monte Carlo Error Rate for Abend-Fritchman Channel Model, $D = 0$

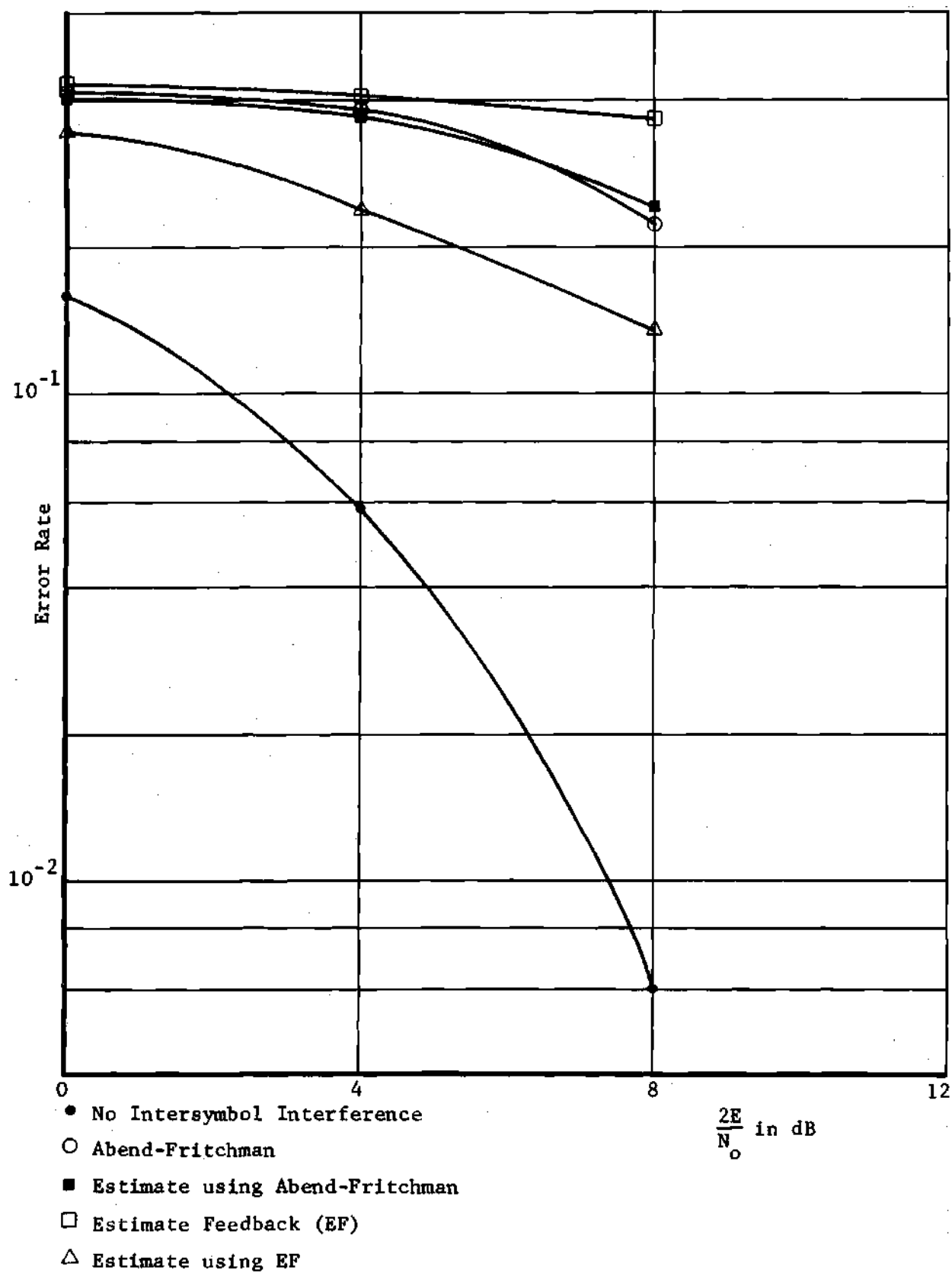


Figure 12. Monte Carlo Error Rate for Abend-Fritchman Channel Model, $D = 1$

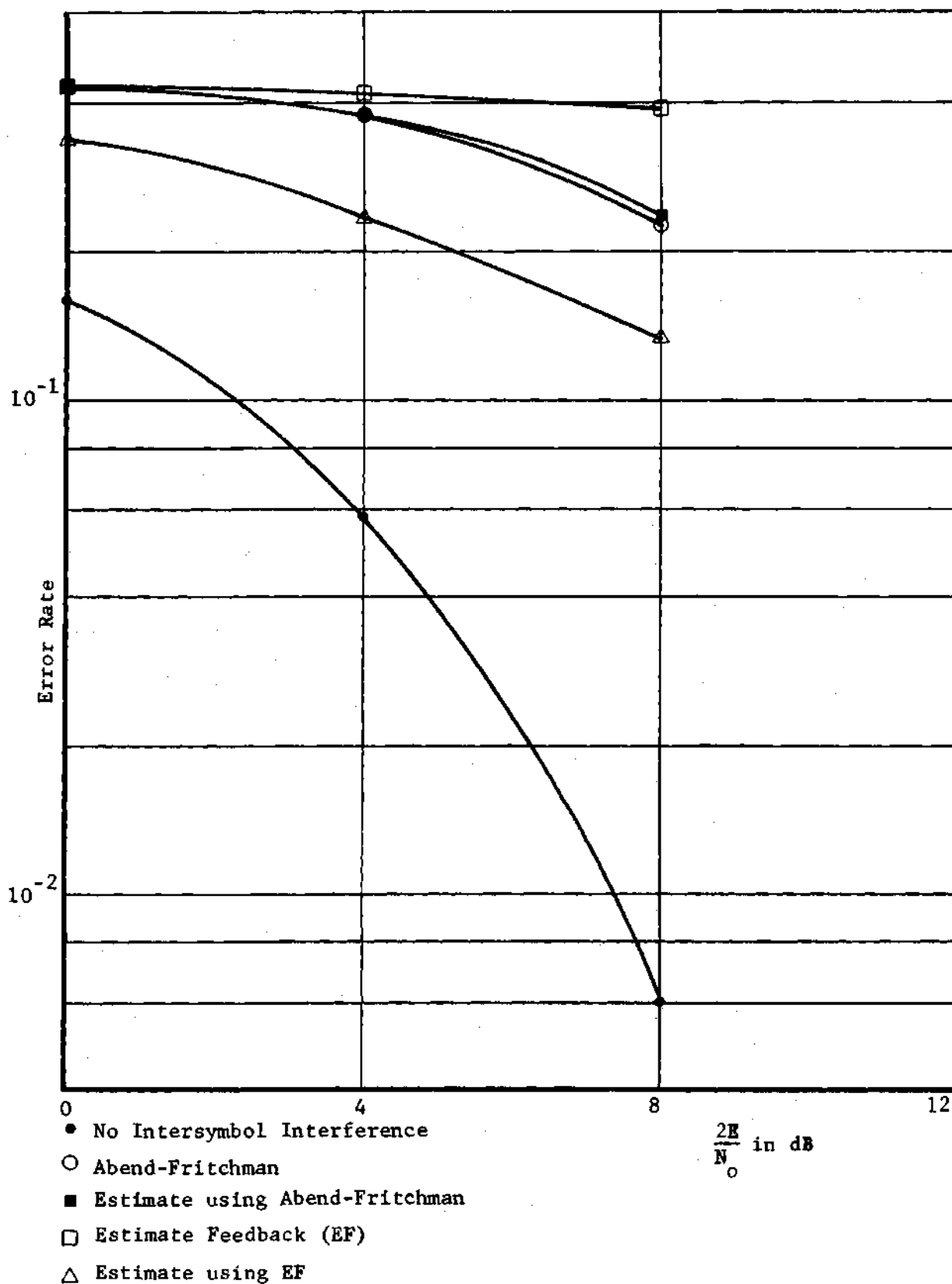


Figure 13. Monte Carlo Error Rate for Abend-Fritchman Channel Model, $D = 2$

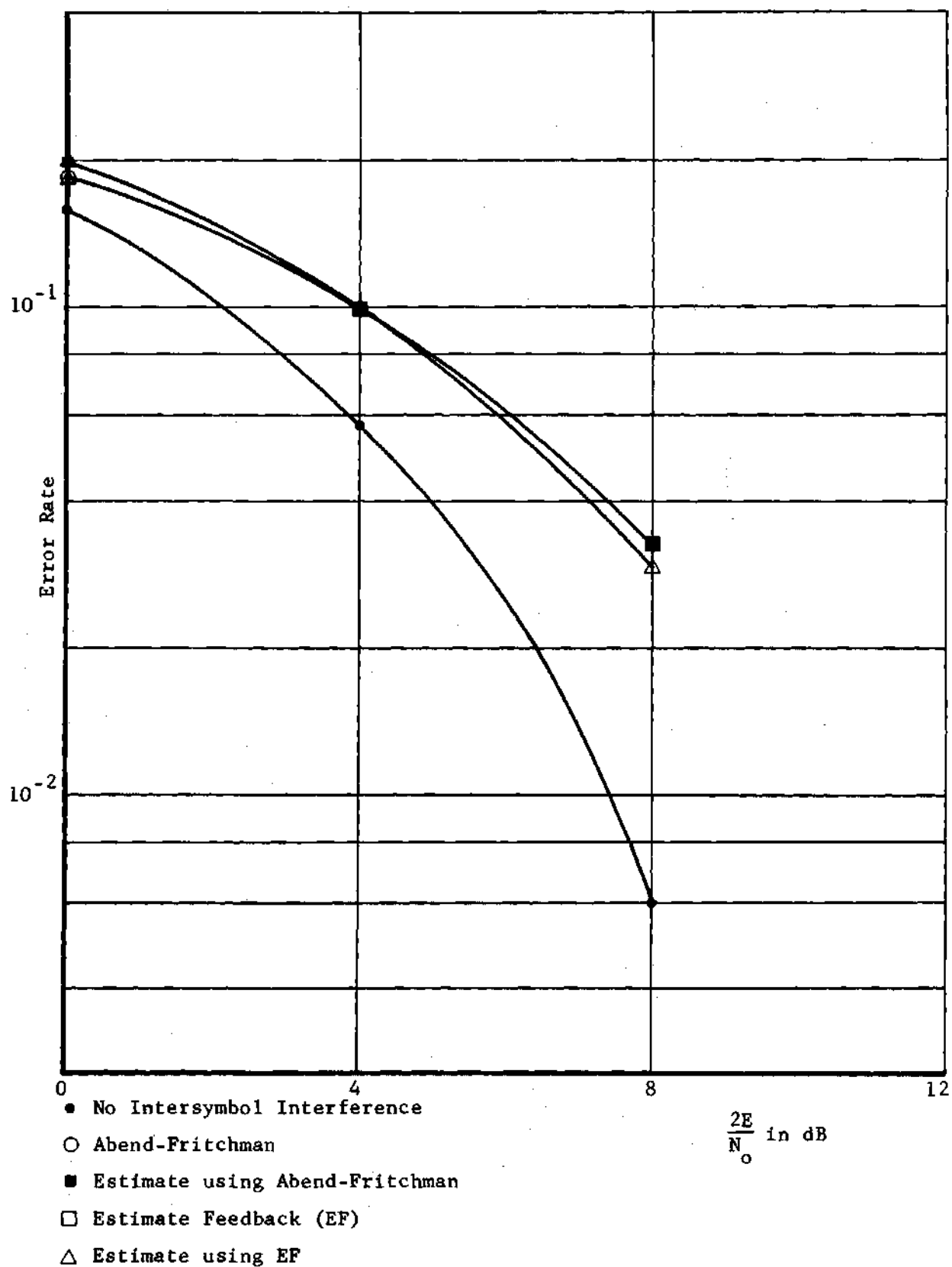


Figure 14. Monte Carlo Error Rate for Abend-Fritchman Channel Model, $D = 3$

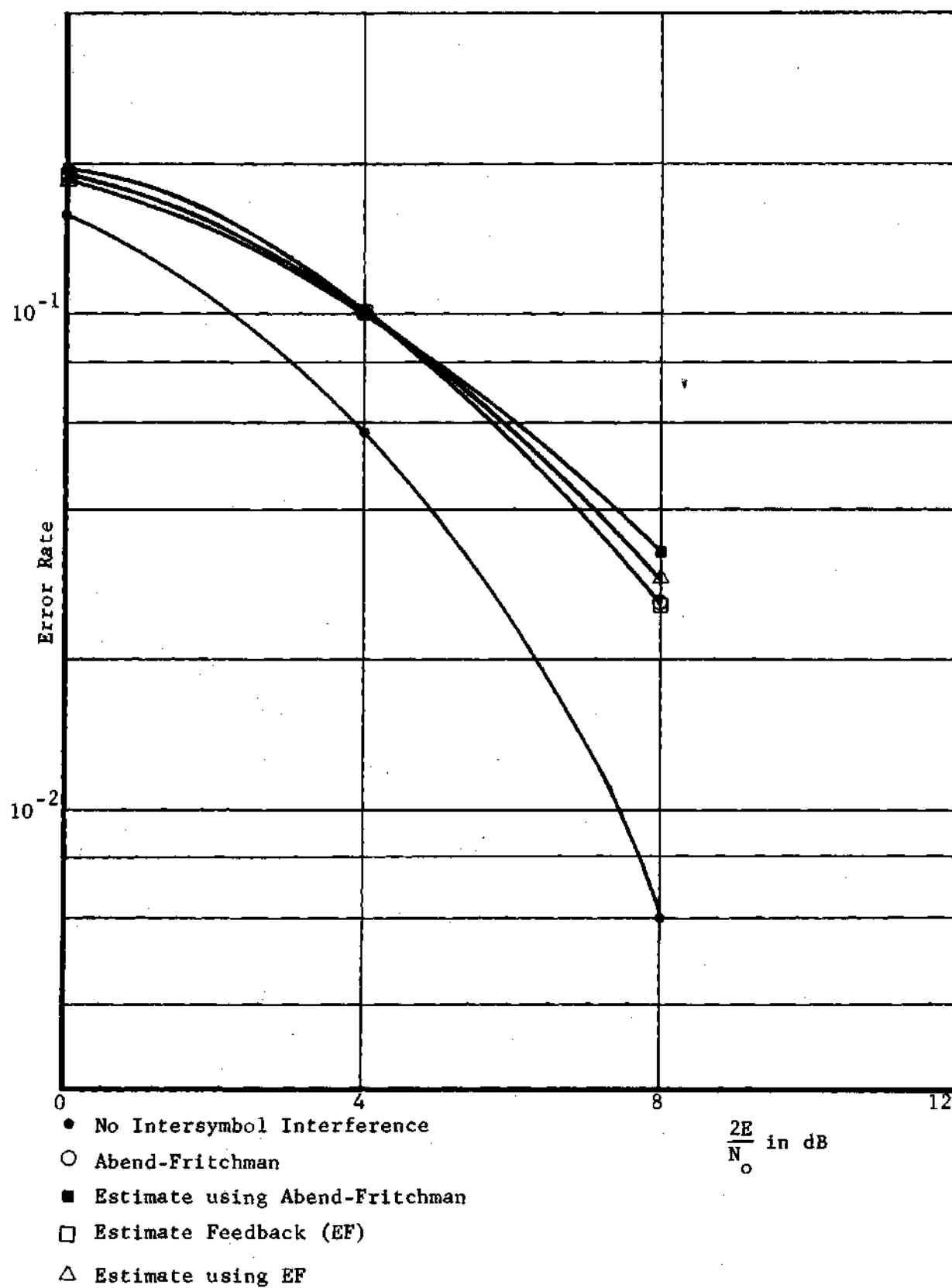


Figure 15. Monte Carlo Error Rate for Abend-Fritchman Channel Model, D = 4

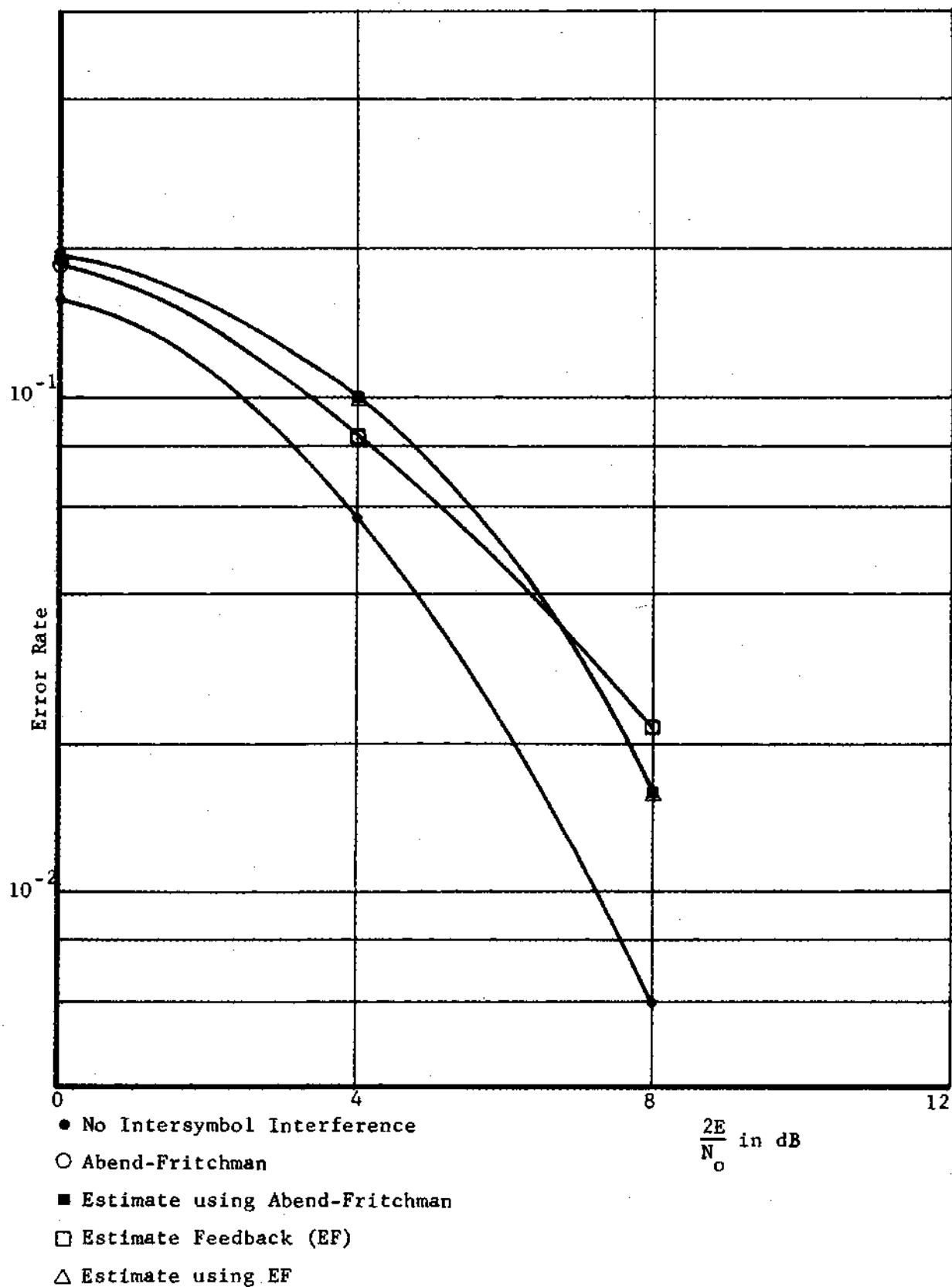


Figure 16. Monte Carlo Error Rate for Abend-Fritchman Channel Model, $D = 5$

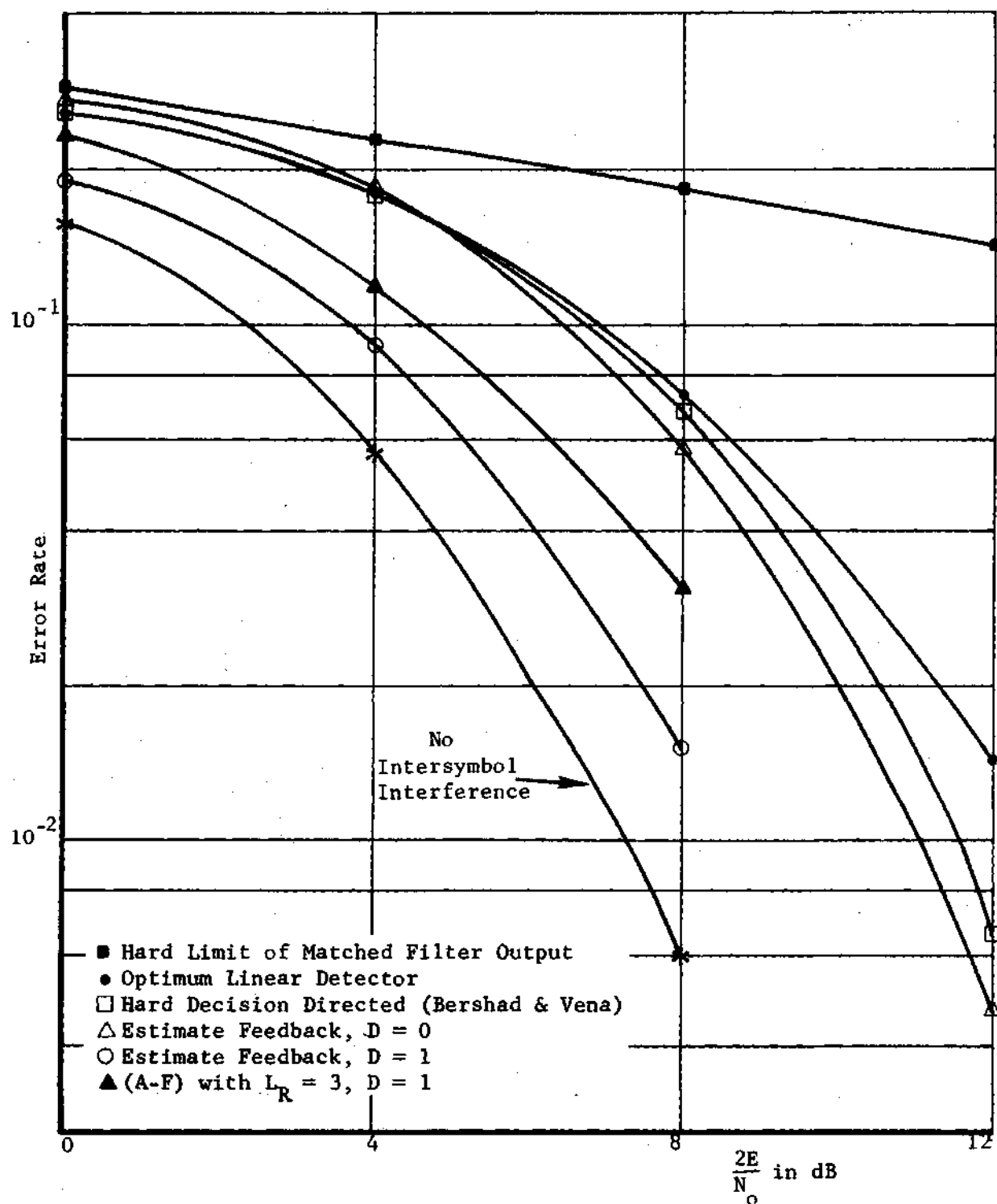


Figure 17. Monte Carlo Error Rates for One Pole Butterworth Channel Model with $f_{co} \approx 1/2\pi$ and $T = 1$; Comparative Results for a Number of Detectors

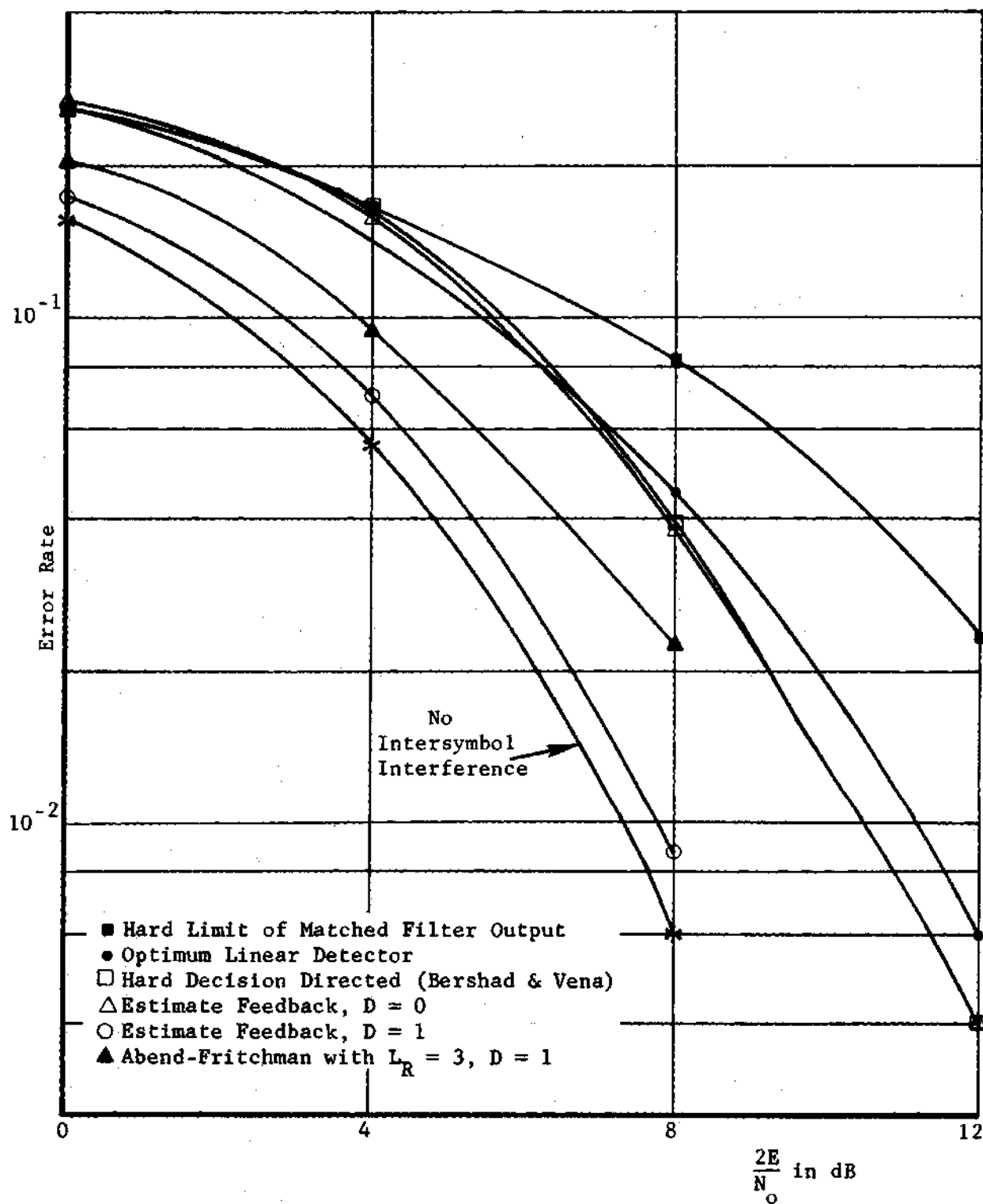


Figure 18. Monte Carlo Error Rates for Two Pole Butterworth Channel Model with $f_{co} = .5$ and $T = 1$; Comparative Results for a Number of Detectors

2. a linear detector that uses a steady state Kalman type of estimator similar to one used in Lawrence and Kaufman [3],
3. a hard decision directed detector that feeds back decisions rather than estimates,
4. an A-F detector using a truncated channel output response of length 3 and delay $D = 1$.
5. estimate feedback detectors with delays $D = 0, 1$.

In these figures one can see the advantage gained by using a rather complex detector such as the A-F or the estimate feedback detector over simple detectors such as the hard limiter. The advantage that the estimate feedback detector has over a detector of the A-F type is also made clear in Figures 17 and 18. The estimate feedback detector for $D = 1$ uses half as many sequence probabilities as the A-F detector with $L = 3$ yet has up to 1 dB better performance.

CHAPTER V

CONCLUSIONS AND RECOMMENDATIONS

Conclusions

This dissertation presents a new suboptimum detector for detecting digital data being transmitted over a WGN channel with memory. The salient features of the algorithm are that:

1. The decision can be postponed to obtain better performance and the trade between performance and complexity is clearly evident.
2. The detector is nonlinear for good performance at high SNR.
3. The detector feeds posterior probabilities, in the form of a hedged decision, back for good performance at low SNR.
4. The algorithm can be applied to channels with either FDIR or state variable models.
5. The algorithm generates a measure of performance with a very slight increase in complexity.

In addition, a pair of discrete time equations is derived that allows an A-F type of detector to be used with any linear, time-varying carrier or baseband channel whose memory is represented by a state variable model, and with any modulation scheme for which all signaling waveforms belong to a linear space.

By simulation of three specific channels the estimate feedback detector developed here is shown to exhibit performance that approaches the no memory case at moderate to high SNR.

Recommendations

There are a number of extensions of this research that should be studied.

In the analytical area it would certainly be desirable to analyze the error rate performance of the detector, possibly relating the mean square error of the symbol estimate to the error rate of the detector. In addition the error rate estimate should be analyzed.

In the area of learning with and without a teacher, it would be a significant contribution to make this algorithm adaptive to the extent that it could learn channel filter parameters as well as signal parameters and noise statistics.

APPENDIX A

SUFFICIENT STATISTICS FOR THE INTERSYMBOL
INTERFERENCE PROBLEMIntroduction

In this appendix a set of sufficient statistics for the intersymbol interference problem is developed. Only the time-invariant case is considered. First, consider the memoryless WGN channel problem. Wozencraft and Jacobs [23] derive a set of sufficient statistics for this problem, and the gist of their argument is as follows:

The detector is assumed to be designed for minimum probability of symbol error. There are M possible signaling waveforms, and all are assumed to belong to a Hilbert space S_s of dimension $N_s \leq M$ and associated interval T .

Since S_s is a finite dimensional linear space, a set of N_s linearly independent basis functions exists such that any $s(t) \in S_s$ can be written as the finite sum

$$s(t) = \sum_{i=1}^{N_s} S_i b_i(t) . \quad (A1.1)$$

This basis set is assumed to have been orthonormalized using the Gram-Schmidt procedure.

The noise, however, lies in an infinite dimensional space S_u , and an infinite number of basis functions are required to write the expansion

$$n(t) = \sum_{i=1}^{\infty} n_i b_i(t) . \quad (A1.2)$$

It can be shown [23] that for WGN, for any choice of basis set, n_i and n_j are statistically independent for $i \neq j$. A convenient choice here is the set consisting of the orthonormal basis set for the signal space, augmented by an infinite number of orthonormal square integrable functions such as to make the basis complete (i.e., that every sample function of $n(t)$ over an interval of length T has a representation in terms of the basis). The specific selection of the augmenting functions is of no concern here.

Recall from Hilbert space theory that knowledge of the coefficients x_i is completely equivalent to knowledge of the corresponding $x(t) \in S_x$, where S_x is any finite or infinite dimensional space; the waveform can be obtained from the coefficients by the series (A1.1) or (A1.2), and the coefficients can be obtained from the waveform by the inner product

$$\langle b_j(t), x(t) \rangle = \langle b_j(t), \sum_{i=1}^{N_s} x_i b_i(t) \rangle . \quad (A1.3)$$

The inner product is linear so that

$$\langle b_j(t), x(t) \rangle = \sum_{i=1}^{N_s} x_i \langle b_j(t), b_i(t) \rangle , \quad (A1.4)$$

and orthonormality implies

$$\langle b_j(t), x(t) \rangle = x_j . \quad (A1.5)$$

This inner product for S_x can be written either as a correlation or a filtering operation

$$\langle x_1(t), x_2(t) \rangle = \int_0^T x_1(t) x_2(t) dt, \quad (A1.6)$$

or

$$\langle x_1(t), x_2(t) \rangle = \int_0^T x_2(t) \bar{x}_1(T-t) dt. \quad (A1.7)$$

The argument is then made that a set of sufficient statistics for this problem is the set of coefficients of $r(t) = s(t) + n(t)$ along the signal space basis. Two facts support this:

1. The only portion of $r(t)$ that depends on the signal is that part lying in S_s .
2. The portion of $r(t)$ not lying in S_s contains only noise, and this noise is statistically independent of the noise in S_s since $n(t)$ is WGN. Consequently the noise energy lying outside S_s is irrelevant to the decision and may be removed with no loss of signal information.

Sufficient Statistics for State Variable Channels

Consider now the extension of the above arguments to the case of a WGN, state variable channel model. The dynamical model for the filter is

$$\dot{\underline{x}}(t) = \underline{F}_c \underline{x}(t) + \underline{G}_c u(t), \quad (A1.8)$$

$$y(t) = \underline{H}_c \underline{x}(t), \quad (A1.9)$$

NOTE: $\bar{x}_1(T-t) \triangleq x_1(t)$.

where $\underline{x}(t)$ is the state of the channel and $y(t)$ is the channel filter output. The filter output can be written for an input pulse in $[0, T]$,

$$y(t) = H_c \phi(t - (k-1)T) \underline{x}((k-1)T) + H_c \int_{(k-1)T}^t \phi(t-\tau) \underline{G}_c u(\tau) d\tau, \quad (A1.10)$$

$$(k-1)T < t < kT,$$

where ϕ is the state transition matrix for the channel. The first term represents the zero input response for the k^{th} signaling interval; that is, it is a function of all symbols through the $(k-1)^{\text{th}}$ as summarized by the channel state at the end of the $(k-1)^{\text{th}}$ interval. The second term in (A1.10), the zero state response, depends on the k^{th} symbol since

$$u(\tau) = \underline{u}'(t - (k-1)T) \underline{u}_k, \quad (k-1)T < t < kT. \quad (A1.11)$$

The sufficient statistics for this problem can be obtained by making a Karhunen-Loeve expansion for $r(t)$, retaining only those coefficients that depend on $y(t)$ and discarding components with noise only. Any set of basis functions will produce statistically independent w_i so that the form of $y(t)$ dictates the choice. The representation developed here is based upon properties of the solution to the linear state equation.

It is known [26] that all zero input responses, namely all solutions to the homogeneous equation,

$$\dot{\underline{x}}(t) = F_c \underline{x}(t), \quad (A1.12)$$

form an N_h dimensional linear space. Thus a basis set $\{b_i^h(t)\}_{i=1}^{N_h}$ for the space exists.

Let $\{b_i^s(t)\}_{i=1}^{N_s}$ be a set of N_s basis functions for the signal space

and let $\{y_i^p(t)\}_{i=1}^{N_s}$ be the zero state responses corresponding to $\{b_i^s(t)\}_{i=1}^{N_s}$.

The members of $\{y_i^p(t)\}_{i=1}^{N_s}$ are in many cases linearly dependent.

Consider now the composite set S_c given by

$$S_c = \{b_i^h\}_{i=1}^{N_h} \cup \{b_i^s(t)\}_{i=1}^{N_s}. \quad (A1.13)$$

A set of N ($N_h \leq N \leq N_s$) linearly independent functions, denoted

$$\{b_i^c(t)\}_{i=1}^N, \quad (A1.14)$$

can always be generated from S_c . These functions form a basis set for a Hilbert space over $[0, T]$ which includes the collection of all channel filter output waveforms as a subset. The set of all outputs is not a linear space, but the need here is to be able to expand any channel output in a finite series.

The set of basis functions can be correlated with a T second segment of $r(t)$, the observation, to produce a vector of sufficient statistics.

Sufficient Statistics for FDIR Channels

In this section the sufficient statistics for the FDIR channel model are developed for completeness. The results are the same as in [16].

The response of an FDIR channel to a given pulse is a waveform $g(t)$ of finite duration and the "chips" of $g(t)$ are defined as

$$g_i(t) = g(t + (i-1)T), \quad i = 1, \dots, L, \quad 0 \leq t < T, \quad (A1.15)$$

so that

$$g(t) = \sum_{i=1}^L g_i(t - (i-1)T). \quad (A1.16)$$

$g_1(t)$ is the zero state response of the filter and the remainder of the chips represent the zero input response of the filter--representing the interference portion of the waveform.

Any possible filter response over $[(k-1)T, kT]$ can be written

$$y(t) = \sum_{i=1}^L u_{k-i} g_i(t). \quad (A1.17)$$

The chips may form a linearly dependent set, but a linearly independent set can be obtained from them. A set of N orthonormal basis functions

$\{b_i(t)\}_{i=1}^N$ over the interval $[0, T]$ can then be generated using the Gram-

Schmidt procedure. Then any channel filter output can be written

$$y(t) = \sum_{i=1}^L y_i b_i(t). \quad (A1.18)$$

Again, an information lossless way of sampling the input data is to use a bank of filters, each matched to a member of $\{b_i(t)\}$.

APPENDIX B

PROBABILITY OF ERROR FOR THE OPTIMUM DETECTOR

In this appendix a probability of symbol error expression in terms of posterior probabilities is derived for the optimum (minimum probability of error) detector. A special case is developed in [25].

Consider the set of all possible observations L_{k+D} , denoted by S . The M posterior probabilities,

$$p(\underline{u}_k = \underline{A}_i | L_{k+D}), \quad i = 1, \dots, M, \quad (B1.1)$$

generated by the optimum detector are defined over S .

The universe S is partitioned by the detector into M disjoint subsets, S_i , such that

$$p(\underline{u}_k = \underline{A}_i | L_{k+D}) \geq p(\underline{u}_k = \underline{A}_j | L_{k+D}) \quad (B1.2)$$

for $i \neq j$ and $L_{k+D} \in S$.

The conditional error probability is

$$p(\epsilon | \underline{u}_k = \underline{A}_i) = \int_{S_i^c} p(L_{k+D} | \underline{u}_k = \underline{A}_i) dL_{k+D}, \quad (B1.3)$$

where S_i^c is the complement of S_i in S . The total error probability is then

$$P_e = \sum_{i=1}^M p(\epsilon | \underline{u}_k = \underline{A}_i) p(\underline{u}_k = \underline{A}_i) \quad (B1.4)$$

$$= \sum_{i=1}^M p(\underline{u}_k = \underline{A}_i) \int_{S_i^c} p(L_{k+D} | \underline{u}_k = \underline{A}_i) dL_{k+D}, \quad (B1.5)$$

$$= \sum_{i=1}^M \int_{S_i^c} p(L_{k+D}, \underline{u}_k = \underline{A}_i) dL_{k+D}, \quad (B1.6)$$

$$= \sum_{i=1}^M \int_{S_i^c} p(\underline{u}_k = \underline{A}_i | L_{k+D}) p(L_{k+D}) dL_{k+D}, \quad (B1.7)$$

where the last step results from Bayes Rule.

In the special case of $M = 2$,

$$P_e = \int_{S_1^c} p(\underline{u}_k = \underline{A}_1 | L_{k+D}) p(L_{k+D}) dL_{k+D} + \int_{S_2^c} p(\underline{u}_k = \underline{A}_2 | L_{k+D}) p(L_{k+D}) dL_{k+D}, \quad (B1.8)$$

$$= \int_S \min_i \{p(\underline{u}_k = \underline{A}_i | L_{k+D})\} p(L_{k+D}) dL_{k+D}, \quad (B1.9)$$

$$= E_{L_{k+D}} [\min_i p(\underline{u}_k = \underline{A}_i | L_{k+D})]. \quad (B1.10)$$

APPENDIX C

THE ESTIMATE FEEDBACK ALGORITHM

The estimate feedback detector generates

$$\hat{p}(\underline{u}_k = \underline{A}_i / L_{k+D}), \quad i = 1, \dots, M, \quad (C1.1)$$

and makes the decision,

$$d(\underline{u}_k) = \underline{A}_j, \quad (C1.2)$$

$$\text{if } \hat{p}(\underline{u}_k = \underline{A}_j) \geq \hat{p}(\underline{u}_k = \underline{A}_i), \quad i = 1, \dots, M. \quad (C1.3)$$

The probabilities (C1.1) are generated from summing sequence probabilities,

$$\hat{p}(\underline{u}_k = \underline{A}_i / L_{k+D}) = \sum_{\underline{u}_{k+1}} \dots \quad (C1.4)$$

$$\sum_{\underline{u}_{k+D}} \hat{p}(\underline{u}_k = \underline{A}_i, \underline{u}_{k+1}, \dots, \underline{u}_{k+D} / L_{k+D}), \quad i = 1, \dots, M,$$

where each summation is taken over M possible symbols. The sequence probabilities are obtained from

$$\hat{p}(u_k = \underline{A}_i, u_{k+1}, \dots, u_{k+D}/L_{k+D}) = \quad (C1.5)$$

$$\hat{p}(\tilde{l}_{k+D}/u_k = \underline{A}_i, u_{k+1}, \dots, u_{k+D}, L_{k+D-1}) \cdot \hat{p}(u_k = \underline{A}_i,$$

$$u_{k+1}, \dots, u_{k+D}/L_{k+D-1}) \div \hat{p}(\tilde{l}_{k+D}/L_{k+D-1}) \quad i = 1, \dots, M.$$

The denominator is identical for all $i = 1, \dots, M$ and can be considered as a normalization factor C . In this work an independent symbol sequence has been assumed, so that,

$$\hat{p}(u_k = \underline{A}_i, u_{k+1}, \dots, u_{k+D}/L_{k+D-1}) = \quad (C1.6)$$

$$\hat{p}(u_k = \underline{A}_i, u_{k+1}, \dots, u_{k+D-1}/L_{k+D-1}) \cdot \hat{p}(u_{k+D}), \quad i = 1, \dots, M.$$

Then (C1.5) becomes

$$\hat{p}(u_k = \underline{A}_i, u_{k+1}, \dots, u_{k+D}/L_{k+D}) = C \hat{p}(u_{k+D}). \quad (C1.7)$$

$$\hat{p}(\tilde{l}_{k+D}/u_k = \underline{A}_i, u_{k+1}, \dots, u_{k+D}, L_{k+D-1}) \cdot$$

$$\hat{p}(u_k = \underline{A}_i, u_{k+1}, \dots, u_{k+D-1}/L_{k+D-1}), \quad i = 1, \dots, M.$$

The last term of (C1.7) can be rewritten so that

$$\hat{p}(u_k = \underline{A}_i, u_{k+1}, \dots, u_{k+D}/L_{k+D}) = \quad (C1.8)$$

$$C \cdot \hat{p}(\underline{u}_{k+D}) \cdot \hat{p}(\tilde{\underline{l}}_{k+D}/\underline{u}_k = \underline{A}_1, \underline{u}_{k+1}, \dots, \underline{u}_{k+D}, \underline{L}_{k+D-1}) \cdot$$

$$\sum_{\underline{u}_{k-1}} \hat{p}(\underline{u}_{k-1}, \dots, \underline{u}_{k+D-1}/\underline{L}_{k+D-1}), \quad i = 1, \dots, M.$$

The third term in (C1.8) is a Gaussian density, whose mean, $\tilde{\underline{l}}_k^m$, is obtained by using the state and observation recursions,

$$\hat{\underline{x}}_{k-1}^c = \hat{\underline{x}}_{k-1}, \quad (C1.9)$$

$$\hat{\underline{x}}_j^c = \tilde{F}_j \hat{\underline{x}}_{j-1}^c + \tilde{G}_j \underline{u}_j, \quad j = k, \dots, k+D, \quad (C1.10)$$

$$\tilde{\underline{l}}_{k+D}^m = \tilde{H}_{k+D}^1 \hat{\underline{x}}_{k+D-1}^c + \tilde{H}_{k+D}^2 \underline{u}_{k+D}, \quad (C1.11)$$

$$\hat{\underline{u}}_k = \sum_{i=1}^M \underline{A}_i \hat{p}(\underline{u}_{k-1} = \underline{A}_i/\underline{L}_{k+D-1}), \quad (C1.12)$$

$$\hat{\underline{x}}_k = \tilde{F}_k \hat{\underline{x}}_{k-1}^c + \tilde{G}_k \hat{\underline{u}}_k \quad (C1.13)$$

and whose variance is the additive noise variance.

The last term in (C1.8) is available from the previous iteration of the recursion. The recursion occurs in the order

$$\hat{\underline{x}}_{k-1}^c = \hat{\underline{x}}_{k-1}, \quad (C1.9)$$

$$\hat{\underline{x}}_j^c = \tilde{F}_j \hat{\underline{x}}_{j-1}^c + \tilde{G}_j \underline{u}_j, \quad j = k, \dots, k+D, \quad (C1.10)$$

$$\hat{p}(\underline{u}_k = \underline{A}_1, \underline{u}_{k+1}, \dots, \underline{u}_{k+D}/L_{k+D}) = \quad (C1.8)$$

$$c \cdot \hat{p}(\underline{u}_{k+D}) \cdot \hat{p}(\underline{\tilde{L}}_{k+D}/\underline{u}_k = \underline{A}_1, \underline{u}_{k+1}, \dots, \underline{u}_{k+D}, L_{k+D-1}) \cdot$$

$$\sum_{\underline{u}_{k-1}} \hat{p}(\underline{u}_{k-1}, \dots, \underline{u}_{k+D-1}/L_{k+D-1}), \quad i = 1, \dots, M,$$

$$\hat{p}(\underline{u}_k = \underline{A}_1/L_{k+D}) = \sum_{\underline{u}_{k+1}} \dots \quad (C1.4)$$

$$\sum_{\underline{u}_{k+D}} \hat{p}(\underline{u}_k = \underline{A}_1, \underline{u}_{k+1}, \dots, \underline{u}_{k+D}/L_{k+D}), \quad i = 1, \dots, M,$$

$$\hat{u}_k = \sum_{i=1}^M \underline{A}_i \hat{p}(\underline{u}_{k-1} = \underline{A}_i/L_{k+D-1}), \quad (C1.12)$$

$$\hat{x}_k = \tilde{F}_k \hat{x}_{k-1} + \tilde{G}_k \hat{u}_k. \quad (C1.13)$$

BIBLIOGRAPHY

1. T. Ericson, "Structure of optimum receiving filters in data transmission systems," IEEE Trans. Inform. Theory (Corresp.), Vol. IT-17, May 1971, pp. 352-353.
2. M. R. Aaron and D. W. Tufts, "Intersymbol interference and error probability," IEEE Trans. Inform. Theory, Vol. IT-12, Jan. 1966, pp. 26-34.
3. R. E. Lawrence and H. Kaufman, "The Kalman filter for the equalization of a digital communications channel," IEEE Trans. Commun. Technol., Vol. COM-19, Dec. 1971, pp. 1137-1141.
4. T. Berger and D. W. Tufts, "Optimum pulse amplitude modulation, Part I: Transmitter-receiver design and bounds from information theory," IEEE Trans. Inform. Theory, Vol. IT-13, Apr. 1967, pp. 196-208.
5. J. M. Aein and J. C. Hancock, "Reducing the effects of intersymbol interference with correlation receivers," IEEE Trans. Inform. Theory, Vol. IT-9, July 1963, pp. 167-175.
6. D. A. George, "Matched filters for interfering signals," IEEE Trans. Inform. Theory (Corresp.), Vol. IT-11, Jan. 1965, pp. 153-154.
7. D. W. Tufts, "Nyquist's problem--The joint optimization of transmitter and receiver in pulse amplitude modulation," Proc. IEEE, Vol. 53, Mar. 1965, pp. 248-259.
8. E. E. Newhall, S. U. H. Qureshi, and C. F. Simone, "A technique for finding approximate inverse systems and its application to equalization," IEEE Trans. Commun. Technol., Vol. COM-19, Dec. 1971, pp. 1116-1127.
9. R. W. Chang and J. C. Hancock, "On receiver structures for channels having memory," IEEE Trans. Inform. Theory, Vol. IT-12, Oct. 1966, pp. 463-468.
10. M. E. Austin, "Decision feedback equalization for digital communication over dispersive channels," M.I.T. Res. Lab Elect., Tech. Rep. 461, Aug. 1967.

BIBLIOGRAPHY (Continued)

11. N. J. Bershad and P. A. Vena, "Eliminating intersymbol interference --A state-space approach," IEEE Trans. Inform. Theory, Vol. IT-18, Mar. 1972, pp. 275-281.
12. D. P. Taylor, "Nonlinear feedback equalizer employing a soft limiter," Electronics Letters, Vol. 7, May 1971, pp. 265-267.
13. D. P. Taylor, "The estimate feedback equalizer: a suboptimum nonlinear receiver," IEEE Trans. Commun., Vol. COM-21, Sept. 1973, pp. 979-990.
14. J. W. Mark, "Comments on 'The estimate feedback equalizer: a suboptimum nonlinear receiver,'" IEEE Trans. Commun., Vol. COM-22, June 1974, p. 885.
15. K. Abend and B. D. Fritchman, "Statistical detection for communication channels with intersymbol interference," Proc. IEEE, Vol. 58, May 1970, pp. 779-785.
16. G. D. Forney, Jr., "Maximum-likelihood sequence estimation of digital sequences in the presence of intersymbol interference," IEEE Trans. Inform. Theory, Vol. IT-18, May 1972, pp. 363-378.
17. K. Abend, T. J. Harley, Jr., B. D. Fritchman, and C. Gumacos, "On optimum receivers for channels having memory," IEEE Trans. Inform. Theory (Corresp.), Vol. 14, Nov. 1968, pp. 819-820.
18. R. R. Bowen, "Bayesian decision procedure for interfering digital signals," IEEE Trans. Inform. Theory (Corresp.), Vol. IT-15, July 1969, pp. 506-507.
19. R. A. Gonsalves, "Maximum-likelihood receiver for digital data transmission," IEEE Trans. Commun. Technol., Vol. COM-16, July 1968, pp. 392-398.
20. G. Ungerboeck, "Nonlinear equalization of binary signals in Gaussian noise," IEEE Trans. Commun. Technol., Vol. COM-19, Dec. 1971, pp. 1128-1137.
21. G. Ungerboeck, "Adaptive maximum-likelihood receiver for carrier-modulated data-transmission systems," IEEE Trans. Commun., Vol. COM-22, May 1974, pp. 624-636.
22. E. C. Thiede, "Decision hysteresis reduces digital P_e ," IEEE Trans. Commun., Vol. COM-20, Oct. 1972, pp. 1038-1041.

BIBLIOGRAPHY (Concluded)

23. J. M. Wozencraft and I. M. Jacobs, Principles of Communication Engineering, John Wiley & Sons, Inc., New York, 1965.
24. G. A. Ackerson and K. S. Fu, "On state estimation in switching environments," IEEE Trans. Automat. Contr., Vol. AC-15, Feb. 1970, pp. 10-16.
25. M. E. Hellman and J. Raviv, "Probability of Error, Equivocation, and the Chernoff Bound," IEEE Trans. Inform. Theory, Vol. IT-16, July 1970, pp. 368-372.
26. L. A. Zadeh and C. A. Desoer, Linear System Theory: The State Space Approach, McGraw-Hill Book Co., Inc., New York, 1963.
27. A. Papoulis, Probability, Random Variables, and Stochastic Processes, McGraw-Hill, New York, 1965.
28. L.-N. Lee, "Real-Time Minimal-Bit-Error Probability Decoding of Convolutional Codes," IEEE Trans. Commun., Vol. COM-22, Feb. 1974, pp. 146-151.

VITA

John Kenna Roach, III, son of John Kenna Roach, II and Daisy McCoy Roach, was born in Paintsville, Kentucky, January 2, 1945. He graduated from Inez High School, Inez, Kentucky, in 1962. He entered the University of Kentucky and in 1966 received the B.S.E.E. degree. Thereupon he was awarded a National Defense Education Act Fellowship to pursue the doctoral degree at the Georgia Institute of Technology. In 1968 he received the M.S.E.E. In 1969 he was appointed to a Graduate Teaching Assistantship in the School of Electrical Engineering.

In November, 1968, Mr. Roach married the former Julia Bradfield Roach of Midway, Kentucky. They presently have one daughter, Susan Kenna.

Mr. Roach is a member of Eta Kappa Nu, Tau Beta Pi, Pi Mu Epsilon, Omicron Delta Kappa, and the Institute of Electrical and Electronic Engineers.